Deltares

Modelling sand-mud interaction in Delft3D

Investigation of sand-mud modules in Delft3D and Delft3D-FM

Modelling sand-mud interaction in Delft3D
Investigation of sand-mud modules in Delft3D and Delft3D-FM

Author(s)
Ana Colina Alonso
Roy van Weerdenburg
Bas van Maren
Ymkje Huismans

Modelling sand-mud interaction in Delft3D
Investigation of sand-mud modules in Delft3D and Delft3D-FM

Client	SO Programme Resilient Ecosystems
Contact	Ana Colina Alonso
Reference	
Keywords	Sand-mud interaction, Delft3D

Document control	
Version	0.1
Date	18-12-2020
Project number	11203754-001
Document ID	11205286-010-ZWS-0001
Pages	66
Status	final

Author(s)		
	Ana Colina Alonso	
	Roy van Weerdenburg	
	Bas van Maren	
	Ymkje Huismans	

Doc. Version	**Author**	**Reviewer**	**Approver**	**Publish**
0.1	Ana Colina Alonso	Thijs van Kessel	Toon Segeren	
	Roy van Weerdenburg			
	Bas van Maren			
	Ymkje Huismans			

Summary

Estuaries and tidal basins are unique systems that are often under pressure by increasing human activities and climate change. In many of these systems the contribution from both sand and mud are essential in their response to measures and global change, i.e. their resilience. For complexity reasons, sand and mud are often treated separately or only one fraction is regarded, despite various studies showing the considerable effect of sand-mud interaction on morphodynamics.

This study, funded by the Deltares Research program “Resilient Ecosystems”, has been performed to improve morphodynamic modelling by integrating the computation of sand and mud transport in Delft3D. It furthermore investigates how the interaction of sand and mud influences the morphodynamic development of tidal basins consisting of mixtures of both sediment types.

Three ways to include (physical) sand-mud interaction are implemented in Delft3D, namely:

- Making use of β_m, in combination with the sand transport formulations of van Rijn (1984, 1993, 2007). An increased value of β_m (for 0 to 1 or 3) is used to simulate the effect of an increased threshold for erodibility of sand when the mud content increases.
- The theory of van Ledden (2003), which accounts for two regimes within sand-mud mixtures, either non-cohesive or cohesive. Sand and mud erosion are interdependent within the two regimes.
- The effect of the bed roughness (depending on the sediment composition) on the bed shear stress acting on sediment particles can be accounted for by using the method of Soulsby & Clarke (2005) to calculate the bed shear-stress generated by waves and currents.

We have provided a detailed description of the implementation of these formulations in Delft3D, as well as their underlying physical meaning. The implemented options for sand-mud interaction have been tested with simulations of a schematised tidal basin, and their effects on short- and long-term simulation results have been evaluated.

In short term-simulations, accounting for sand-mud interaction (all 3 types discussed above) can change the predicted erosion rates significantly. Besides, it is shown that changing the settings for sand-mud interaction largely affects the predicted long-term morphological evolution, and the (local and general) bed sediment composition. In general, transitions between sandy and muddy areas are sharper when accounting for sand-mud interaction. In addition, a bimodal distribution of the mud content (which has been observed in the intertidal flats of the Western Scheldt and the Wadden Sea) can be reproduced. This bimodality is most distinct when accounting for the effect of the bed roughness as defined by Soulsby & Clarke (2005).

This work shows that including sand-mud interaction is essential to determine the future fate of deltas, since it largely influences their long-term development, altering bed level evolution and sediment composition as explained above. With that it contributes to the new mission area “Future Deltas”. In addition, including sand-mud interaction is key for future studies on sustainable sediment management, ecology and water quality, as it influences the sand-mud distribution, turbidity and erosion rates. These findings are relevant for the mission area “Sustainable Deltas”.

Content

List of Symbols

Symbol	Unit	Description
Roman symbols		
D_{50}	µm	Median grain size diameter
D_{sand}	µm	User-specified sand grain size
D_*	-	Dimensionless grain size
$E_{fm,i}$	m/s	Erosion velocity of pure mud for mud fraction i
E_m	m/s	Erosion of mud
$E_{m,i}$	m/s	Erosion velocity of cohesive mud for fraction i
E_s	m/s	Erosion of sand
$E_{sm,i}$	m/s	Erosion velocity for mud fraction i in the non-cohesive regime
g	m/s^2	Gravitational acceleration
k_s	m	Nikuradse roughness length
M_c	m/s	Erosion parameter in the cohesive regime
M_e	m/s	Erosion parameter for (100%) mud
M_{nc}	m/s	Erosion parameter in the non-cohesive regime
p_{si}	-	Silt content
p_{cl}	-	Clay content
p_m	-	Mud content
$p_{m,cr}$	-	Critical mud content
T_{nc}	-	Transport parameter (van Ledden, 2003)
u_{*e}	m/s	Effective friction velocity
z_0	m	Bed roughness length
Greek symbols		
$\alpha_{\beta 1}$	-	Coefficient depending on the transport parameter (van Ledden, 2003)
$\alpha_{\beta 2}$	-	Coefficient depending on the transport parameter (van Ledden, 2003)
β_m	-	Erodibility coefficient
γ	-	Coefficient (van Rijn, 2007)
Δ	-	Specific density of sand
θ_{cr}	-	Critical Shields parameter
ρ_s	kg/m^3	Sediment density
ρ_w	kg/m^3	Water density
τ_b	Pa	Bed shear stress
τ_{cr}	Pa	Critical shear stress for erosion of sand
τ_e	Pa	Critical shear stress for erosion of mud
$\tau_{e,c}$	Pa	Critical shear stress for erosion of a sand-mud mixture in the cohesive regime
$\tau_{e,nc}$	Pa	Critical shear stress for erosion of a sand-mud mixture in the non-cohesive regime
$\phi_{cohesive}$	-	Coefficient for cohesive particle-particle interaction
$\phi_{packing}$	-	Coefficient for packing effects
φ	°	Phase

1 Introduction

1.1 Background

The sediment composition of the bed is an important characteristic of coastal and estuarine environments. It governs sediment mobility, hence sediment transport and morphological evolution. Estuaries and tidal basins all over the world are unique systems that are often under pressure by increasing human activities and climate change. In many of these systems the contribution from both sand and mud are essential in their response to measures and global change, i.e. their resilience. Examples are floodplain restoration, sediment management around hydropower dams, the morphodynamic development of the Wadden Sea, ecological development (fish, algae) and the response of systems to relative sea level rise. For complexity reasons, sand and mud are often treated separately or only one fraction is regarded, despite various studies showing the considerable effect of sand-mud interaction on morphodynamics (e.g. Van Ledden (2003); Winterwerp & Van Kesteren (2004); Jacobs (2011)).

This study was initiated to improve morphodynamic modelling by integrating the computation of sand and mud transport. Several formulations exist in literature describing the combined sand-mud transport, and some of them are (partly) implemented in Delft3D. This study explores some of the interaction mechanisms available in literature, describes how they are implemented in Delft3D, and provides results of numerical experiments evaluating the contribution of several interaction formulations.

1.2 Objectives

The aim of this study is to investigate how the interaction of sand and mud influences the morphodynamic development of tidal basins consisting of mixtures of sand and mud. This objective constitutes the following subtasks:

- Evaluation of methods available to quantify the interaction of sand and mud in process-based morphodynamic models;
- Testing and improvement of these functionalities in Delft3D;
- Quantifying the effect of interactions on long-term morphodynamic development;
- Validation with field observations.

1.3 Outline

The outline of this report is as follows: In Chapter 2, the main theories and general understanding of sand-mud interaction are discussed. Different methods to include sand-mud interaction in Delft3D are introduced in Chapter 3. Both the original methods and how these methods are implemented in Delft3D are discussed. In Chapter 4, these methods are applied in simulating the morphodynamic development of a schematized tidal system. The different sand-mud interaction methods are tested by considering the initial morphodynamic response in the tidal basin. The effects on the morphodynamic development are considered by simulating 50 years of morphodynamic development. A discussion on the results is included in Chapter 5. Finally, the conclusions from this study are included in Chapter 6.

2 Sand-mud interaction: theory and understanding

2.1 Mixed beds

Sediment bed mixtures consisting of mud (particles and flocs < 63 µm) and sand are known as sand-mud mixtures and are generally found along marine and estuarine beds, banks and coasts. Sand-mud bed mixtures are mixtures with appreciable fractions of clay, silt and sand.

The clay fraction of mud-sand beds has cohesive properties and can retain water (Torfs, Erosion of mud/sand mixtures., 1995). Cohesion is caused by van der Waals forces and /or organic polymers binding the very fine plate-type clay particles. The ability of clay to retain water is related to the relatively strong bonding forces between the water molecules and the surface of the fine clay particles, and because of the very fine pores in the clay resulting in very low permeability values. The fine particles consist of various clay and quartz minerals (very fine silt). The most important clay minerals are kaolinite, illite and montmorillonite (subclass of smectites).

Bed deposits formed in sedimentary environments often have layered structures due to differential settling and sediment sorting. Each layer may have a different structure, bulk density (degree of consolidation) and strength against erosion resulting in a stepwise erosional behaviour. Generally, the topmost layer is a thin muddy layer as the very fine particles will settle at the end of the settling process. The upper muddy layer generally is soft and can be easily eroded if it is freshly deposited. The mud particles will almost immediately be suspended, when the flow-induced bed-shear stress exceeds the critical shear stress for erosion. A sandy sub-layer underneath a thin mud layer will be eroded as bed load transport with ripple features occurring. Other more consolidated mud layers underneath sand layers may have a much higher erosion strength due to consolidation processes.

Homogeneously mixed sediment beds of clay, slit and sand particles are rare in nature. A typical example of a rather homogeneously mixed bed is the bed surface of an intertidal flat exposed to waves due to the active reworking of the bed surface by the surface waves and bioturbation by benthic organisms.

2.2 Network structure

Cohesive effects in mud-sand mixtures become important in the case that the sand particles are fully surrounded by fine cohesive particles. At low mud contents, the soil structure is dominated by the sand skeleton, as all sand particles are still in contact (see Figure 2.1). At higher mud content, the sand particles are no longer in contact. The structure of the bed is dominated by the clay-water matrix, and the bed has cohesive properties.

For natural mixed sediment beds, the critical clay-silt content (< 63 µm) is estimated at $p_{si,cr}+p_{cl,cr}=p_{mud,cr} \approx 0.3$ (Torfs, 1995; Van Ledden, 2003; van Rijn, Colina Alonso, & van Maren, 2020). A fully space-filling network will be present for clay-silt contents > 30%. The distance between the sand particles will increase for increasing clay-silt content. If the mud content is below the critical value ($p_m<p_{m,cr}$), the bed only has weak cohesive or non-cohesive properties.

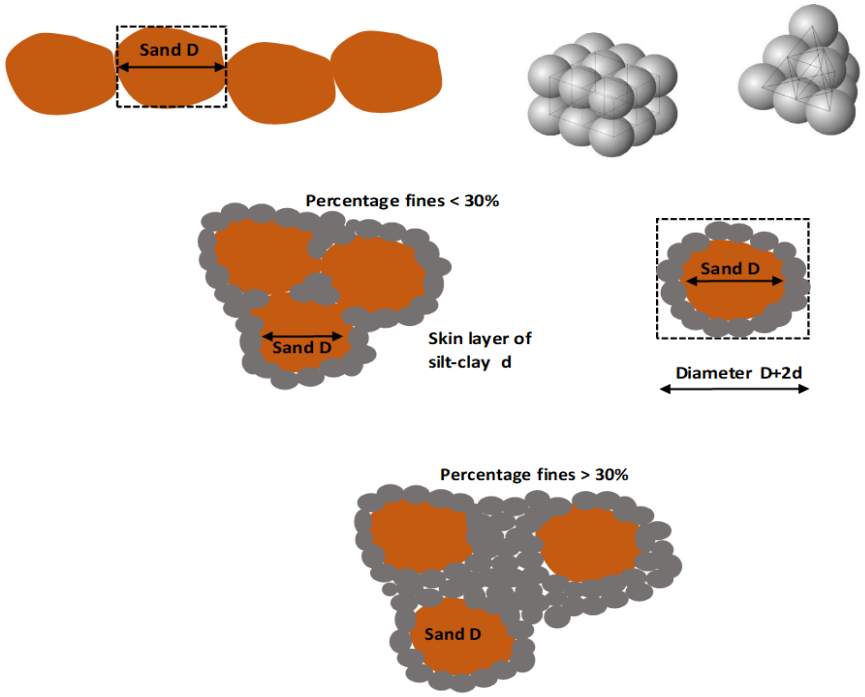

Figure 2.1 Network structures of mud-sand mixtures. Upper: sand particles without mud. Middle: sand particles with skin layer of silt-clay particles (percentage fines < 30%). Lower: sand particles drowned in mud particles (percentage fines > 30%). From: van Rijn, et al. (2020).

2.3 Mud availability in the sediment bed

Fine-grained sediments tend to migrate from high-energy areas (channels) to low-energy areas (flats), and therefore many flats are muddy whereas channels are sandy. In the Wadden Sea for instance, the overall sediment distribution is characterized by a strong sand-mud segregation (Van Straaten & Kuenen, 1957; de Glopper, 1967; Zwarts, 2004; Van Ledden, Sand-mud segregation in estuaries and tidal basins, 2003). The central parts of the basins mainly consist of sandy channels with low (< 10%) mud content. The shoals consist of mixtures of fine sand (with a D_{50} of about 160 µm) and mud. Relatively high mud contents are found close to the mainland coasts, in the Dollard and Balgzand area, across the tidal divides and, to a limited extent, in some patches close to the southern shore of the islands close to saltmarshes. (Herman, et al., 2018).

Herman, et al. (2018) performed an analysis of the SIBES dataset (2008-2013, covering all intertidal areas of the Dutch Wadden Sea including the Ems-Dollard estuary) and found that the Wadden Sea environments tend to be either mud-dominated or sand-dominated: The statistical distribution of the values of %mud (<63 µm) shows a clear bimodality with many low observations (range 2-7 %, mode 4.5 %) and many high observations (range 20-50 %, mode 35 %), but fewer observations in between. A comparison with data of the Sediment Atlas Wadden Sea showed that this bimodality has remained relatively stable in the past decades, as indicated in Figure 2.2. A similar bimodality is found for the shoals of the Western Scheldt based on data by McLaren (1994), see Figure 2.3.

Besides, Herman, et al. (2018) showed that stations with a mean close to the modes of the statistical distribution (either low or high) are relatively stable in time, whereas the more rare observations with a mean in between the modes tend to have a higher standard deviation. They suggest that this reflects the stability of the different states, where both modes can be characterized as stable conditions, whereas in between the modes instability is more likely.

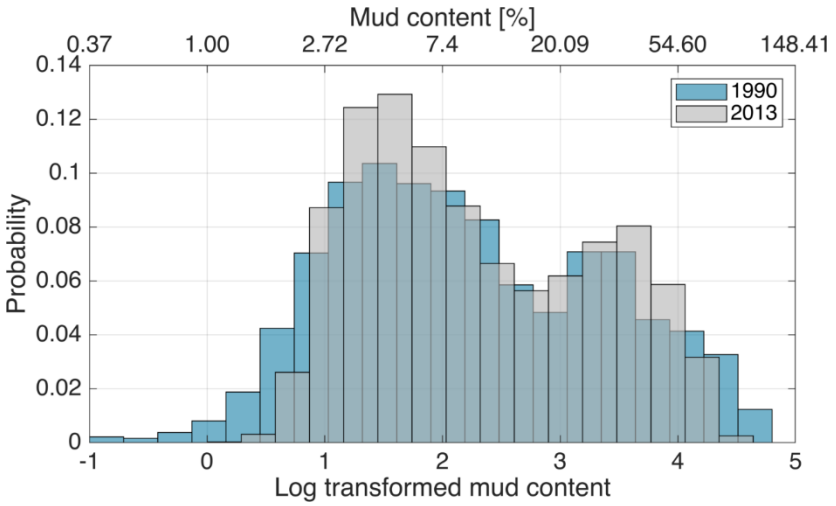

Figure 2.2 Bimodality of the mud content in the sediment bed showing the distribution based on SIBES data (2013) and Sediment Atlas data (1990) including bed samples of intertidal areas only. From: (Colina Alonso, 2020)

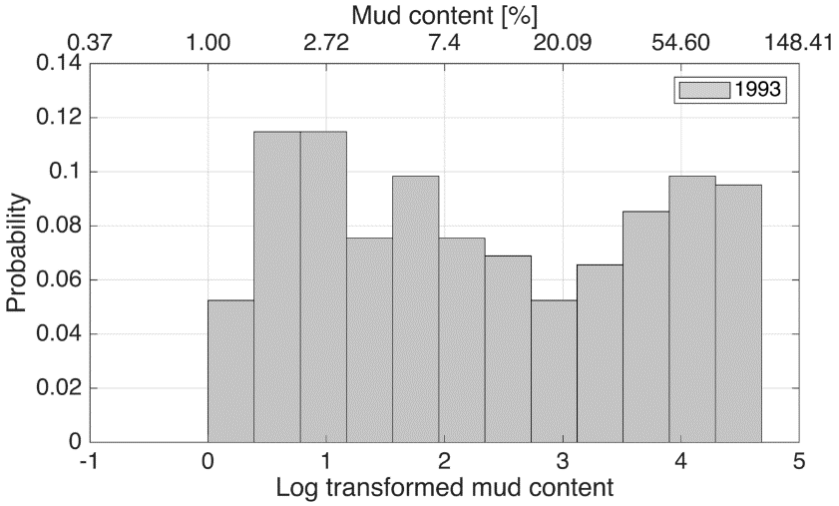

Figure 2.3 Distribution of the mud content in the intertidal areas of the Western Scheldt, based on data by McLaren (1994).

A correlation exists between the maximum bed shear stress and the mud content in the sediment bed. Field data of the Wadden Sea reveal the existence of a threshold for the bed shear stress: above this value, the bed consists of mainly sand with a very low mud content. Below this value, a large scatter in the mud content is observed. Often, a sharp transition between these regimes is observed and a critical transition value can be defined. De Bake (2000) found similar results at the Molenplaat in the Western Scheldt (see Figure 2.4). Van Ledden (2003) established an equilibrium value for the mud content at the bed surface, based on the (critical) bed shear stresses, and the deposition and erosion capacity. He concluded that sharp transitions exist when the mud deposition capacity is low (e.g. low suspended mud concentration) and showed that the transitions are expected to be more gradual for higher values of the mud concentration.

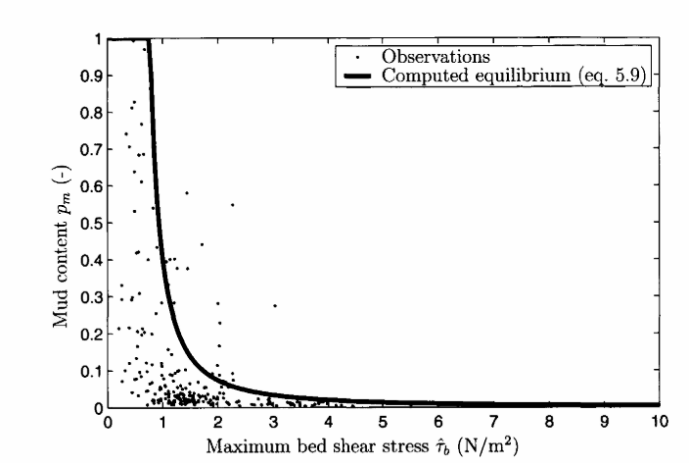

Figure 2.4 Correlation between observed mud content and maximum bed shear stress (De Bake, 2000) and derived equilibrium mud content (Van Ledden, 2003) against maximum bed shear stress for Molenplaat area.

2.4 Effect of sand-mud interaction on erodibility

Several experiments have demonstrated that the erosion characteristics can change dramatically when small amounts of mud are added to a sand bed ((Bisschop, 1993; Mitchener & Torfs, 1996). For example, Torfs (1995) measured a 2–5 times higher critical erosion shear stress than the critical shear stress for pure sand when 10% mud was added to the sand bed. Besides, the erosion rate strongly decreased with increasing mud content. According to van Ledden, et al. (2004) , this suggests that the erosion behavior of sand–mud mixtures cannot be described by using the existing erosion formulations for pure sand (Van Rijn, 1993; Soulsby R. , 1997) or pure mud (Winterwerp, 1989; Whitehouse, Soulsby, & Mitchener, 2000).

Based on experiments, Torfs (1995) showed that a critical amount of mud exists at which sand grains loose contact and a mud matrix covers the sand particles (see also Section 2.2). Below this critical mud content, the mixture can be treated as cohesionless sediment, while above cohesive forces determine the erosive behavior of the mixture. Torfs also showed that the critical content is a function of the sand grain size, the type of cohesive material, the clay fraction and the organic content. In addition, van Ledden, et al. (2004) explain that the cohesiveness of a natural sediment bed not only increases with increasing clay content by dry weight, but also with decreasing water content. Besides they show that the transition between non-cohesive and cohesive behavior ranges between 5% and 10% clay content for Dutch systems. Assuming an average critical clay content of 7% and a clay/silt ratio of 0.24 (as is the case for the bed sediments in the Western Scheldt), this gives a critical mud content of approximately 35%.

Since the erodibility of sand-mud mixtures is dependent on mud content, a positive feedback between the two variables is expected. This might be a mechanism leading to the observed bimodal distribution of the mud content (see Section 2.3). Herman, et al. (2018) namely state that bimodality is often an indicator of a bistable system, where there are two equilibrium states and intermediate states are unstable. Bistability in a system is usually the consequence of positive feedback: once a particular condition is reached, it tends to maintain or strengthen itself in that condition, whereas when the system is flipped over to an alternative state, it tends to stay in that alternative condition.

2.5 Effect of the sediment composition on the bed roughness

Another positive feedback mechanism that might be the cause for the observed bimodality, is related to the effect of the sediment composition on the hydraulic roughness of the bed. The hydraulic roughness of mud beds is lower than of that of sandy beds, since (larger) sand grains generate more near-bed turbulence. Since the bed shear stress increases with the hydraulic roughness, lower bed shear stresses will be exerted on muddy beds. Besides, high concentrations of suspended

matter in the water column generate a reduction of the apparent roughness, as sediment concentration gradients damp vertical mixing by turbulence. Consequently, as the bed becomes muddier, the forces responsible for erosion of fines decrease in strength and chances are that the mud content further increases. However, this mechanism only takes place if the starting conditions are near the critical threshold for mud resuspension (Herman, et al., 2018).

2.6 Ecology and biota

The interaction between bed sediment and ecology is a two-way interaction, although here we restrict ourselves to the effects of biota on sediment dynamics. Many plant and animal species are so-called ecosystem engineers, i.e. organisms whose presence or activity alters the abiotic properties of a habitat (Jones et al., 1994; 1997).

In the past decades many studies have described significant effects of biota on sedimentation and erosion rates of mud, by either stabilizing or destabilizing the sediment. Examples are:

- Marine vegetation enhances the bottom dissipation of current energy and reduces shear stress at the sediment–water interface, which is especially significant when the shoot density is high.
- Microphytobenthos and secreted EPS stabilize the sediment, and an increase of up to a factor of 5 can be assigned to the erosion threshold on muddy beds (e.g. Le Hir et al., 2007; Andersen et al, 2010). The development of benthic diatoms tends to be seasonal, so that stabilising effects are likely to be minimal in winter. Although most studies focus on the surface phenomenon caused by EPS, biogenic stabilization is not necessarily confined to the presence of a surface biofilm: EPS may penetrate the surface of the sediment matrix and establish a vertical profile (Chen et al., 2017). Therefore, after full erosion of the biofilm protection, the high EPS content in the sublayers continues to stabilize the sediment (hindered erosion) by binding individual grains. Consequently, the bed strength does not immediately revert to the abiotic condition.
- Macrofaunal effects are characterized by extreme variability, and they can have two distinct effects on benthic–pelagic exchange (see also Widdows et al., 2000). Their filtration of suspended matter can result in biodeposition of fines (stabilizing effect). However, the bioturbation caused by their movement through the upper sediment layers, can result in a significant increase of the mass eroded once the critical erosion current velocity has been reached (destabilizing effect). For muddy sediments, destabilization seems to be the general trend (Herman et al., 2001; Le Hir et al., 2007).

The former line of thinking was that large-scale morphology of many sand-mud systems (such as the Wadden Sea) is a physical process, and that biota can have a significant effect on the fine sediment dynamics. The exception is saltmarshes, which can trap fine sediment for long timescales and significantly influence large scale morphology (Morris, 2007). However, Borsje et al. (2008) showed that on local spatial scales and at seasonal timescales biota can certainly have a major effect. In addition, le Hir et al. (2007) showed that whereas the effects of the presence of microphytobenthos are only seasonal and have little to no effect on the long-term morphodynamics, vegetation on salt marshes can induce significant seaward shifts of upper flats, that remain present in the long-term.

In this report, we further restrict ourselves to investigating the abiotic components of sand-mud interaction. Nevertheless, it is acknowledged that there can be a strong link between ecology and the physical properties and morphodynamic behaviour of sand-mud environments, both in the short- and the long term.

3 Implemented sand-mud interaction modules

The theoretical framework of three different methods that are implemented in Delft3D to include the interaction of sand and mud particles are discussed in this chapter. For each of the three methods the original framework of formulations is discussed, as well as how these formulations are implemented in Delft3D and how the method can be applied.

3.1 Van Rijn formulations

The sediment transport formulations by Van Rijn (e.g. Van Rijn (1984), Van Rijn (1993) and Van Rijn (2007)) are commonly used in sediment transport computations in general, and in Delft3D modelling in specific. The computation of the critical bed shear stress in these formulations allows for a certain interaction between sand and mud in the sediment bed: Based on the results of various studies, it can be concluded that the erosion or pick-up process of the sand particles is slowed down by the presence of the mud particles. This behaviour can be quite well modelled by increasing the critical bed-shear stress for initiation of motion of the sand particles. Since the implementation is slightly different in the different versions of the Van Rijn formulations, they will be discussed independently.

Van Rijn (1984)
According to the formulations by Van Rijn (1984), the critical bed shear stress for erosion is computed in Delft3D as;

$$\tau_{cr} = (\rho_s - \rho_w) * g * D_{50} * \theta_{cr} * (1 + p_{mud})^{\beta_m} \qquad (2.1)$$

where ρ_s and ρ_w are respectively the density of sediments and the density of water, g is the gravitational acceleration, D_{50} is the median grain size diameter and θ_{cr} is the critical Shields parameter. p_{mud} is the mud fraction in the top layer of the sediment bed and β_m is a user defined variable. The term between brackets is responsible for sand-mud interaction: the critical shear stress for erosion of sand increases with higher mud contents if $\beta_m > 0$. Since β_m is a user defined variable, setting it to 0 would ensure the mud content does not increase the resistance against erosion of sand particles.

The computation that is discussed here is handled in subroutine *tranb7* of the Delft3D source code. The correction factor for the presence of mud in the active layer is not reported in the Delft3D-FLOW User Manual (Deltares, 2018).

Van Rijn (1993)
The sediment transport method following Van Rijn (1993) includes a computation of the critical bed shear stress for erosion of sand that is the same as the one included in Van Rijn (1984). Until recently, the parameter β_m was fixed at 3. From version 6.03.00.65439 (January 2020, changed as part of the present project) of the Delft3D source code onwards, β_m is again a user defined variable. The default value for β_m in Delft3D is 3.

The computations dealing with β_m in the Van Rijn (1993) transport formulations are coded in subroutines *tram1* and *bedbc1993* of the Delft3D source code. The Delft3D-FLOW User Manual (Deltares, 2018) does not mention this interaction mechanism when discussing the sediment transport formulations.

Van Rijn (2007)

Also in the Van Rijn (2007) sediment transport formulations the mud content can be taken into account when computing the critical shear stress for erosion, although in a slightly different manner than in Van Rijn (1993) if the representative sediment size (D_{50}) is smaller than the representative diameter of sand particles. The reasoning behind this is that natural beds of fine sediment generally show cohesive effects (Van Rijn, 2007). The computation is as follows if $D_{50} < D_{sand}$ (where D_{sand} is a user-specified grain size, for which Van Rijn (2007) proposes 62 µm):

$$\tau_{cr} = \phi_{packing} * \phi_{cohesive} * (\rho_s - \rho_w) * g * D_{50} * \theta_{cr} \quad (2.2)$$

in which

$$\phi_{cohesive} = \max\left[\left(\frac{D_{sand}}{D_{50}}\right)^{\gamma}, 1\right]$$

And

$$\phi_{packing} = \min\left[\frac{\min\left[\max\left[\frac{D_{50}}{D_{sand}} * 0.65,\ 0.05\right],\ 0.65\right]}{0.65}, 1\right].$$

γ is a user defined input value in the range of 1-2. If $D_{50} > D_{sand}$, the bed shear stress is computed as in Van Rijn (1993). Also for Van Rijn (2004), the parameter β_m used to be fixed at 3. From version 6.03.00.65439 of the Delft3D source code onwards, β_m is again a user defined variable. The computations dealing with β_m in the Van Rijn (2004) transport formulations are coded in subroutines tram2 and bedbc2004 of the Delft3D source code.

3.2 Van Ledden (2003) with extensions

Based on literature and data-analysis, Van Ledden (2003) assumes that the erosional behaviour of sand-mud mixtures behaves significantly different in two regimes: a non-cohesive and a cohesive one. He proposed a mathematical description for sand-mud mixtures, accounting for this division in two regimes. The transition between the two regimes depends on the clay content; it takes place at a critical clay content ($p_{cl,cr}$) of 5 to 10%. Assuming a constant clay/silt ratio, which is valid for Dutch estuarine systems, a critical mud content ($p_{m,cr}$) can be determined at which the transition takes place.

Note that these formulations apply for the bed layer and not for the fluff layer (when applying them in combination with a buffer-fluff module), as the bed layer has sand-mud interaction and the fluff layer (containing only mud) does not.

Non-cohesive sand-mud mixtures

For non-cohesive sand-mud mixtures ($p_m < p_{m,cr}$), mud is eroded proportionally with sand instead of being eroded individually (which could calculated with for instance the Partheniades-Krone equations). Van Ledden (2003) states that existing equations that relate the relative critical bed shear stress to the mud content (such as the formulations by Van Rijn), largely overestimate the effect of the mud content on the critical shear stress for erosion of non-cohesive sand-mud mixtures. Therefore, he proposes the following relationship;

$$\frac{\tau_{e,nc}}{\tau_{cr}} = (1 + p_m)^{\beta_m} \quad (2.3)$$

where $\tau_{e,nc}$ is the critical shear stress for non-cohesive mixtures, τ_{cr} is the critical shear stress for sand and β_m (set at 0.75-1.25) is an empirical coefficient which may depend on the packing of the bed. Van Ledden (2003) initially combined this method with transport formulations of van Rijn (1984,

1993), and the full implementation in Delft3D can be used with van Rijn formulations only. Braat, et al (2017) used the code of van Ledden (2003) in Delft3D in combination with the sand transport formulation of Engelund & Hansen (1967), but explained that this does not allow for a full implementation of sand-mud interaction, as defined by van Ledden (2003).

The increase in critical bed shear stress for erosion with increasing mud content is shown in Figure 3.1, for different values of β_m according to the formulations of van Ledden and van Rijn. Also, experimental data is included in this figure (circles). It illustrates that determining the right value for β_m is not a trivial task. Van Rijn (1993) proposes to use $\beta_m = 3$, whereas Van Ledden (2003) proposes to use a value between $\beta_m = 0.75$ and $\beta_m = 1.25$, since he aims at obtaining a good fit in the non-cohesive regime (bounded by mud content until 30% approximately). Especially if the mud content increases, a different value for β_m is going to make a large difference in the resistance against erosion.

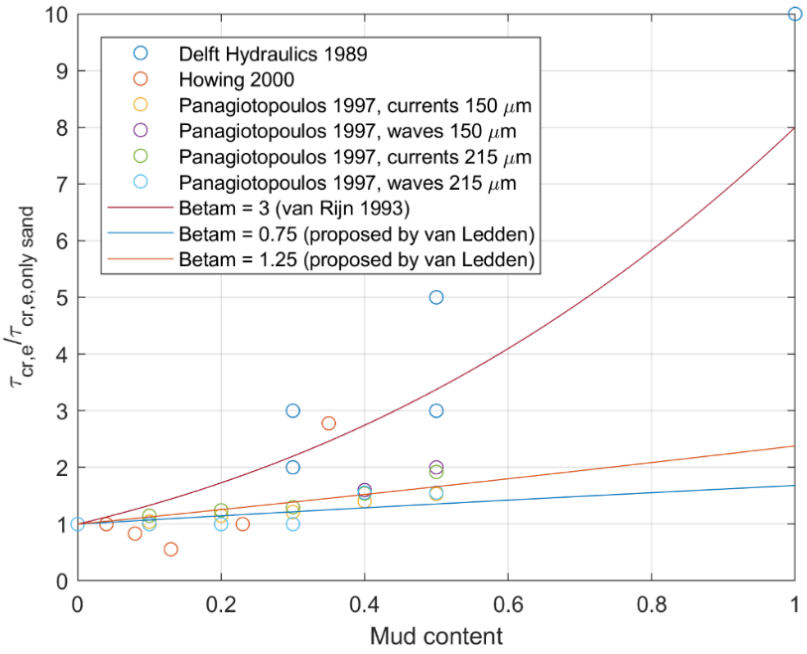

Figure 3.1 Comparison between experimental data and the relationship between the relative critical shear stress of sand and the mud content, as proposed by Van Rijn (1993) and by Van Ledden (2003).

The following formula for the erosion of mud in the non-cohesive regime was derived by Van Ledden (2003);

$$E_m = \frac{\alpha_{\beta 1}}{3}\frac{p_m}{1-p_m}\frac{\sqrt{\Delta g D_{50}}}{D_*^{0.9}} T_{nc}^{\alpha_{\beta 2}-0.9} \qquad (2.4)$$

in which $\alpha_{\beta 1}$ and $\alpha_{\beta 2}$ are coefficients depending on the transport parameter T_{nc}, p_m is the mud content at the bed surface, Δ is the specific gravity of sand, g is the gravitational acceleration, D_{50} is the median sand grain size and D_* is the dimensionless grain size. The reader is referred to Chapter 3 of Van Ledden (2003) for the derivation of Equation 1.5.

The transport parameter T_{nc} includes the modified critical shear stress for non-cohesive mixtures and is defined as;

$$T_{nc} = \frac{\tau_b}{\tau_{cr}(1+p_m)^{\beta}} - 1 \qquad (2.5)$$

Cohesive sand-mud mixtures

The bed becomes cohesive when the mud content in the bed exceeds the critical mud content. The erosive behaviour of such mixtures takes place as suspended transport only; therefore, the bed load transport rate is assumed as $q_b = 0$.

The erosion of sand (E_s) and mud (E_m) are both computed with a Partheniades-type of equation, stating that above a certain critical bed shear stress the cohesive bed starts to erode with an erosion rate M_c. The erosion formulations for both sediment types are as follows:

$$E_s = (1 - p_m) M_c \left(\frac{\tau_b}{\tau_{e,c}} - 1\right) H\left(\frac{\tau_b}{\tau_{e,c}} - 1\right) \quad (2.6)$$

$$E_m = p_m M_c \left(\frac{\tau_b}{\tau_{e,c}} - 1\right) H\left(\frac{\tau_b}{\tau_{e,c}} - 1\right) \quad (2.7)$$

in which $H(\frac{\tau_b}{\tau_{e,c}} - 1)$ is a heaviside function that equals 1 when the argument is larger than 0, and equals 0 when the argument is less or equal to 0. $\tau_{e,c}$ is the critical shear stress for erosion of cohesive sand-mud mixtures which is linearly interpolated between $\tau_{e,nc}$ (the critical bed shear stress for the non-cohesive regime) and τ_e (the critical bed shear stress for a pure mud bed). $\tau_{e,c}$ is defined as

$$\tau_{e,c} = \frac{\tau_{cr}\left(1+p_{m,cr}\right)^{\beta} - \tau_e}{1 - p_{m,cr}} (1 - p_m) + \tau_e \quad (2.8)$$

Likewise, the cohesive erosion coefficient M_c is interpolated between the erosion parameter for the non-cohesive regime M_{nc} and the erosion parameter for the fully mud regime M_e. The expression for the cohesive erosion coefficient M_c reads

$$\log(M_c) = \frac{\log\left(\frac{M_{nc}}{1-p_{m,cr}}\right) - \log(M)}{1 - p_{m,cr}} (1 - p_m) + \log(M) \quad (2.9)$$

in which M is the erosion coefficient for a pure mud bed (ranging from 10^{-3} to 10^{-5}) and the erosion coefficient for non-cohesive mixtures is defined as

$$M_{nc} = \frac{\alpha_{\beta 1}}{3} \frac{\sqrt{\Delta g D_{50}}}{D_*^{0.9}} \quad (2.10)$$

For multiple sand and mud fractions, this approach is mathematically complex since each fraction may have its own value for M_e and M_{nc}. Therefore, Van Kessel, et al. (2012) interpolate the erosion velocity itself (instead of $\tau_{e,c}$ and M_c separately):

$$E_{m,i} = E_{fm,i} \left(\frac{E_{sm,i}}{E_{fm,i}}\right)^{\frac{1-p_m}{1-p_{m,cr}}} \quad (2.11)$$

where $E_{m,i}$ is the erosion velocity of cohesive mud for fraction i, $E_{fm,i}$ is the erosion velocity of pure mud for mud fraction i, and $E_{sm,i}$ is the erosion velocity for mud fraction i in the non-cohesive regime.

Application in Delft3D

The theory by Van Ledden (2003) on the erodibility of sand-mud mixtures is implemented in the Delft3D morphodynamic suite and extended (from one sand- and one mud fraction to multiple fractions), as documented in Van Kessel, et al. (2012) (called in *erosed* (Delft3- FM: *fm_erosed*), which makes use of the subroutine *sand_mud*).

To include this sand-mud interaction in a simulation, the `PmCrit` ($p_{m,cr}$) input variable is required in the *.sed file, such that the top of the *.sed file would for example look like what is listed below.

```
[SedimentOverall]
   Cref             = 1.6000000e+003 [kg/m3]
   IopSus           = 0
   PmCrit           = 0.3
```

In addition, the parameter `Betam` (β_m) can be defined in the *.tra file when the Van Rijn formulations are used to determine the transport of sand.

3.3 Soulsby & Clarke (2005)

Soulsby & Clarke (2005) derived mathematical expressions for the bed shear-stress generated by the combined effects of waves and currents as a function of the bed roughness and hence the turbulent flow regime. In contrast to earlier studies, it describes a method applicable for hydrodynamically rough turbulent flows as well as for hydrodynamically smooth turbulent flows. Sand and gravel beds can often be considered as hydrodynamically rough; muddy beds, and especially freshly-deposited mud beds, can often be considered as hydrodynamically smooth.

In case of hydrodynamically rough turbulent flows, the bed roughness z_0 depends on the surface texture of the sediment bed. A representative grain size (D_{50}) of the sediment is used as a measure for the surface texture:

$$z_0 = \frac{D_{50}}{12} \tag{2.12}$$

In case of the hydrodynamically smooth case, the bed roughness z_0 depends on the kinematic (molecular) viscosity:

$$z_0 = \frac{\nu}{9u_{*e}} \tag{2.13}$$

where u_{*e} is the effective friction velocity. One is referred to the original publication by Soulsby & Clarke (2005) for the full derivation of the expressions.

For the application in modelling sand-mud interaction, the dependence of the bed roughness on the grain size (i.e. Equation 2.12) is most relevant. It implies that the bed roughness is adjusted for changes in sediment composition, such that the bed roughness decreases in case the mud fraction increases (and vice versa). Since the bed shear stress induced by certain hydrodynamic conditions decreases if the bed roughness decreases, the forcing at sediment particles changes with the bed composition. Generally, the stresses induced by certain hydrodynamic conditions are less at more muddy beds than at beds that contain more sand.

Application in Delft3D

The Soulsby & Clarke method to compute bed shear stresses under the combined effect of waves and currents is supported in the Delft3D morphodynamic modelling suite, roughly according to the algorithm in Appendix A of Soulsby and Clarke (2005). The wave orbital motion is based upon H_{rms} and the peak period of the wave spectrum is used as a characteristic wave period. The critical value for the wave Reynolds number is $Re_{w,c} = 1.5 \times 10^5$. The critical value for the current Reynolds number is $Re_{c,cr} = 2000 + (5.92 \times 10^5 + Re_w)^{0.35}$, in which Re_w is the wave Reynolds number.

A difference between the implementation in Delft3D and the original algorithm by Soulsby & Clarke has to do with the definition of the roughness length. In the Soulsby & Clarke method, the roughness length for rough flows is determined as $z_0 = d_{50} / 12$. Herein it is assumed that $k_s = 2.5D_{50}$, where k_s is a Nikuradse roughness length. The characteristic grain size diameter D_{50} is no dependent variable

in Delft3D, such that it is not available to be used to determine z_0. Therefore, a different approach was implemented. In the Delft3D source code the roughness length z_0 (*z0silt* in the source code) is determined as $z_0 = k_s / 30$, where k_s is equal to the k_s value of silt *(ksSilt)* if the amount of mud in the active layer is relatively large and k_s is equal to the k_s value of sand *(ksSand)* if the amount of mud in the active layer is relatively small. Both *ksSilt* and *ksSand* are user defined input parameters.

When applying the Soulsby & Clarke method in Delft3D or Delft3D-FM, the bed shear stress for currents (τ_{hydro}) is still computed based on the form roughness (the overall user-specified bed roughness, either as Chézy, Manning, or White-Colebrook). However, the skin friction instead of the form roughness is used to compute the bed shear stresses (τ_{morph}) based on which the resuspension of sediment is determined. The advantage of this method is that it is physically more realistic (i.e. accounting for smaller-scale variations in the flow and on the bed sediment properties) but also more practical as sediment transport becomes less influenced by hydrodynamic model calibration (e.g. including spatially varying roughness fields).

The Soulsby & Clarke method is applied to compute the bed shear stress from skin friction if `bsskin = true` in the *.sed file. The method is called in the *erosed* routine (Delft3D-FM: *fm_erosed*). Both Delft3D and Delft3D FM then make use of the subroutine *compbsskin* to compute the bed shear stress, based on the algorithm as outlined in Appendix A of Soulsby and Clarke (2005). Input variables necessary to apply the Soulsby & Clarke method are listed below;

- `ksSilt` is the roughness height (in [m]) in case the top layer of the sediment bed mainly consists of mud particles (i.e. smooth beds).
- `ksSand` is the roughness height (in [m]) in case the top layer of the sediment bed mainly consists of sand particles (i.e. rough beds).
- `sc_mudfactor` determines whether the total mud thickness in the active layer or the mud fraction (i.e. by mass) determines the switch between `ksSilt` and `ksSand`. The value should be `#thickness#` or `#fraction#`. The default is `#thickness#` for backward compatibility reasons.
  In mud models (i.e. without simulating a sand fraction) the mud fraction is always equal to unity; therefore, setting `sc_mudfactor = #thickness#` is the only way to change the bottom roughness depending on the amount of mud present in the bed.
- `sc_cmf1` is the lower critical mud factor. Below this value `ksSand` will be used as the roughness height. The default value is 0.01.
- `sc_cmf2` is the upper critical mud factor. Above this value `ksSilt` will be used as the roughness height. The default value is 0.01.

The top of the *.sed file would for example look like what is listed below.

```
[SedimentOverall]
    Cref              = 1.6000000e+003  [kg/m3]
    IopSus            = 0
    bsskin            = true
    ksSilt            = 0.004           [m]
    ksSand            = 0.025           [m]
    sc_mudfactor      = fraction
    sc_cmf1           = 0.3             [-]
    sc_cmf2           = 0.5             [-]
```

A detailed description of the input variables needed to apply the Soulsby & Clarke method in Delft3D is included in the memo that is included in Appendix 1 (Van Weerdenburg, 2020). The settings that are listed above would lead to a relation between the roughness height and the mud fraction in the transport layer as illustrated in Figure 3.2. In case the mud fraction is lower than *sc_cmf1* = 0.3, *ksSand* = 0.025 m is used as the roughness height. In case the mud fraction is higher than *sc_cmf2* = 0.5, *ksSilt* is used as the roughness height. For mud fractions between 0.3 and 0.5, the roughness height follows from an interpolation between *ksSand* and *ksSilt*.

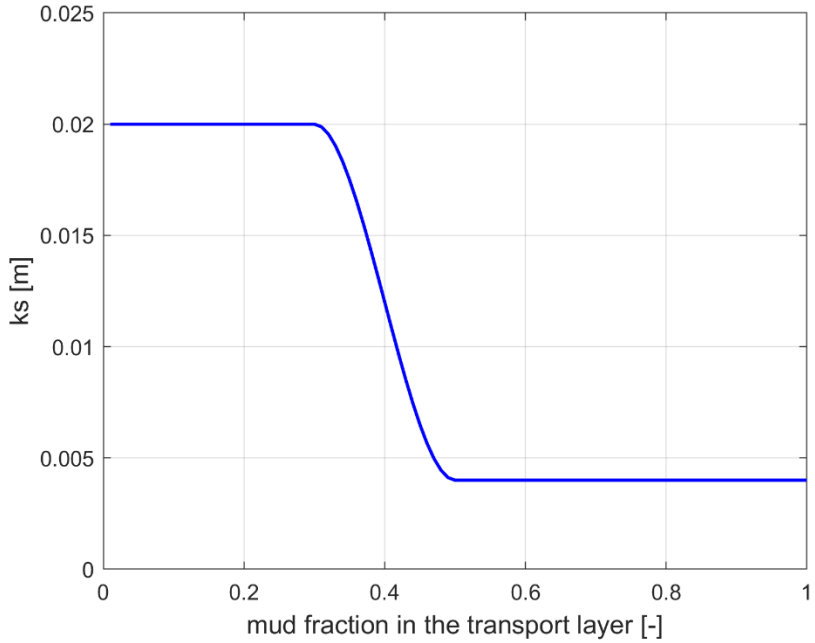

Figure 3.2: Roughness height for a varying mud content in the Soulsby & Clarke method in Delft3D for settings ksSand = 0.02 m, ksSilt = 0.004 m, sc_cmf1 = 0.3 and sc_cmf2 = 0.5.

4 Schematized modelling study

Previous studies have tested the implementation of the theory of van Ledden (2003) in Delft3D for theoretical test cases (1DV model), a Wadden Sea test case and a schematised representation of Ameland tidal basin (van Kessel, et al., 2012; Scheel, 2012). Since we want to enable a comparison between the three sand-mud interaction modules that were discussed in the previous chapter, several modelling exercises have been performed in a schematized model setting. These exercises were intended on the one hand to test whether the modules work correctly, and on the other hand to investigate the effects of applying the modules on the morphodynamic development.

4.1 Model setup

A schematized model of a tidal inlet was set up for this study. The tidal inlet is located between two barrier islands. South of the tidal inlet and the barrier islands is the tidal basin (see Figure 4.1). The computational grid consists of squares of 100 m x 100 m. The model has one open boundary, which is the open sea boundary in the North.

A first version of the model was used to consider the effects of the sand-mud interaction modules on the initial morphodynamic response (i.e. patterns of erosion/sedimentation). These model simulations were also used to see if the modules work correctly. This is easier in a short-term application, since multiple feedback mechanisms (i.e. indirect effects) in a long-term application would make it more difficult to see the direct effects of the modules. Subsequently, the model was adjusted to simulate long-term morphodynamic development. In this long-term application, the effects of the sand-mud interaction modules on morphodynamic development and sand-mud segregation is considered. The two different models (i.e. short-term application and long-term application) are introduced separately.

Short-term application (initial response)
The initial bathymetry of the model for this application is illustrated in Figure 4.1. At the northern model boundary, a semi-diurnal tidal water level variation (i.e. only the S2 component) is prescribed. The amplitude of the water level variation is 1.5 m. In this application, no wave forcing is taken into account. The bottom roughness is determined according to the White-Colebrook formulations, in which the Nikuradse roughness height is set to 0.02 m. The White-Colebrook bed roughness formulations are used to allow for a fair comparison with results of the Soulsby & Clarke (2005) module, in which it is only possible to specify the bed roughness by a Nikuradse roughness height.

The dynamics of two sediment fractions are modelled, namely one sand fraction (median sediment diameter D_{sand} = 150 µm) and one mud fraction (settling velocity w_s = 2.5*10^{-4} m/s). The transport of sand is computed according to the Van Rijn (1993) formulas. The exchange of mud between the water column and the seabed is computed with the Partheniades-Krone formulations (see Deltares (2018)). The initial sediment composition of the seabed varies in different simulations. Initially, there is no sediment in suspension. The critical bed shear stress for erosion of the mud fraction is 0.5 N/m^2 and the erosion speed of the mud fraction is 1*10^{-4} kg/m^2/s. The critical bed shear stress for deposition is set to 0 for the part of the domain offshore of the barrier islands and to 1000 N/m^2 for the remaining part of the domain (i.e. the inlet and the tidal basin), which ensures there is no deposition of mud offshore of the barrier islands. A large amount of mud would otherwise deposit here in many of the simulations, since waves are absent in these model simulations.

The concentration of mud in at the open boundary of the model domain is 5*10^{-3} kg/m^3 for the entire simulation period. The amount of sand coming in from the offshore boundary is equal to the transport capacity for sand at this boundary. The thickness of the transport layer is set to 20 m. By choosing

such a thick transport layer, the bed composition will hardly change during the simulation time. This is necessary to only consider the initial morphodynamic response.

The total simulation time in the short-term application is 24 hours. The first 12 hours are used as the hydrodynamic spin-up time. Morphodynamic changes are computed and processed only in the 2nd 12 hours. No morphological acceleration is applied.

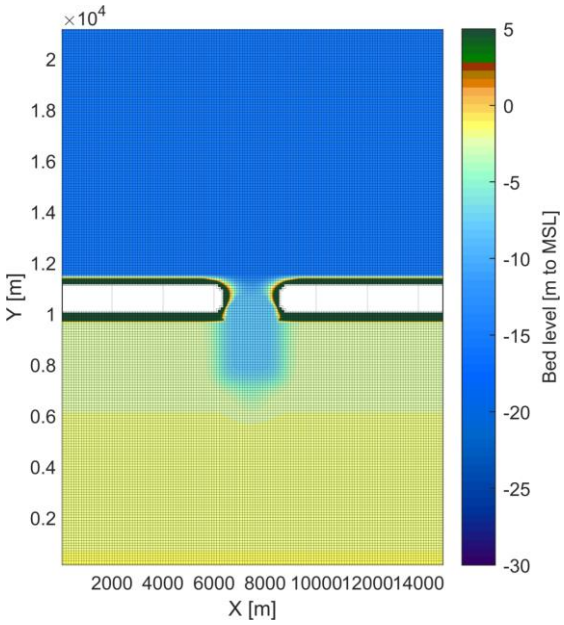

Figure 4.1: Domain and initial bathymetry of the schematized model of a tidal basin in the short-term application. The open sea boundary is at the top of the figure. The other boundaries are closed.

Long-term application (morphodynamic development)

In order to assess the long-term effects of the sand-mud parameterizations, the morphologic development of the same basin was computed for a period of 50 years. Herein a morphological acceleration factor of 50 was applied, which implies that the hydrodynamic simulation time is one year. For this application, the model that was introduced before (i.e. short-term application) was modified in multiple ways:

- The initial bathymetry was modified, such that the bed level decreases gradually from the barrier islands to the offshore boundary (see Figure 4.2).
- The amplitude of the S2 tidal signal at the offshore boundary is set to 1.35 m (φ = 0). In addition, an S4 tidal signal of 0.15 m is prescribed (φ = 180°).
- A wave model (Delft3D-WAVE) is coupled to the model to simulate locally generated wind waves. The wind conditions are such that there is alternating periods with mild, moderate and moderately strong winds from multiple directions. Mild and moderate winds are mainly coming from the southwest, whereas moderately strong winds are comping from the north-western direction.
- The median sediment diameter of the sand fraction (D_{sand}) has been increased to 250 µm. The critical bed shear stress for erosion of the mud fraction has been increased to 1.0 N/m^2. The settling velocity and the erosion speed of the mud fraction are the same as in the short-term application, which is respectively 2.5*10^{-4} m/s and 1*10^{-4} kg/m^2/s.
- The thickness of the transport layer is set to 0.1 m. Below the transport layer, 20 Eulerian sediment layers of 1 m thickness are prescribed. The initial mud fraction in the bed is 5%.
- Both the initial mud concentration in the water and the mud concentration at the open model boundary are set to 5 mg/l.

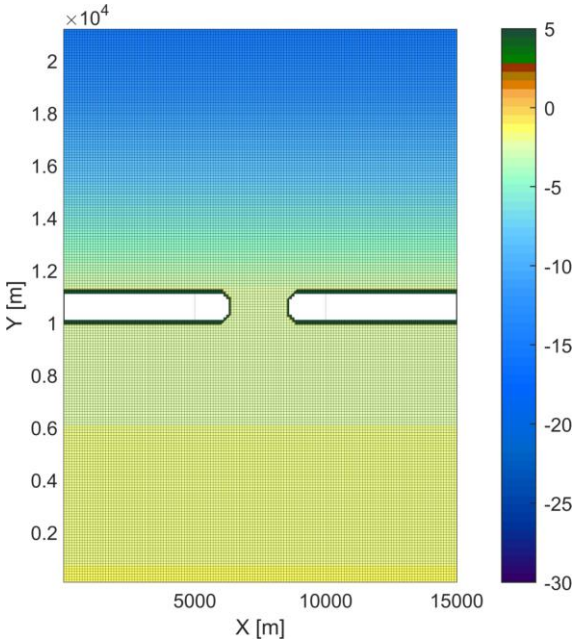

Figure 4.2: Domain and initial bathymetry of the schematized model of a tidal basin in the long-term application. Compared to Figure 4.1, the bed level decreases gradually from the barrier islands to the offshore boundary and there is no initial depth increase around the inlet.

4.2 Short term effects of sand-mud interaction

4.2.1 Van Rijn formulations

As discussed in Paragraph 3.1, the critical shear stress for erosion of the sand fraction depends on the mud fraction if β_m is larger than 0. Figure 4.3 shows the cumulative sedimentation and erosion near the tidal inlet after a morphodynamic simulation of 12 hours, in case the initial mud fraction is set to 5%. In follows from these plot that the morphodynamic changes become smaller by increasing β_m, since the resistance of sand particles against erosion increases.

In case the initial mud fraction increases, the effect of increasing β_m becomes larger. This is illustrated in the plots in Figure 4.4, for which the initial mud fraction was set to 50%. With a mud fraction of 50% and $\beta_m = 3$, the critical shear stress for erosion of sand is $(1 + 0.5)^3 = 3.375$ times as high as the critical shear stress for erosion of sand without the presence of mud. The sediment bed would be relatively stable in this case (see Figure 4.4).

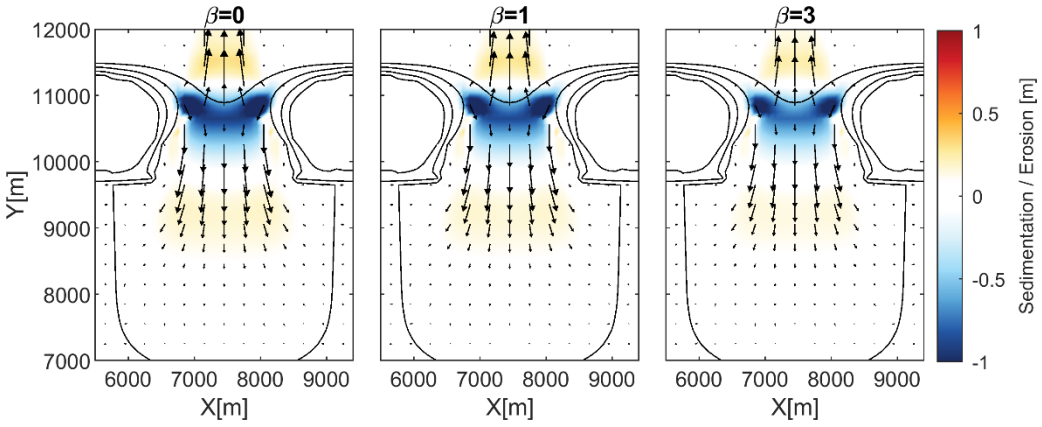

Figure 4.3: Initial morphodynamic response at the inlet with different values for β_m and a homogeneous mud content of 5%. The arrows indicate the residual sediment transport after one tidal cycle.

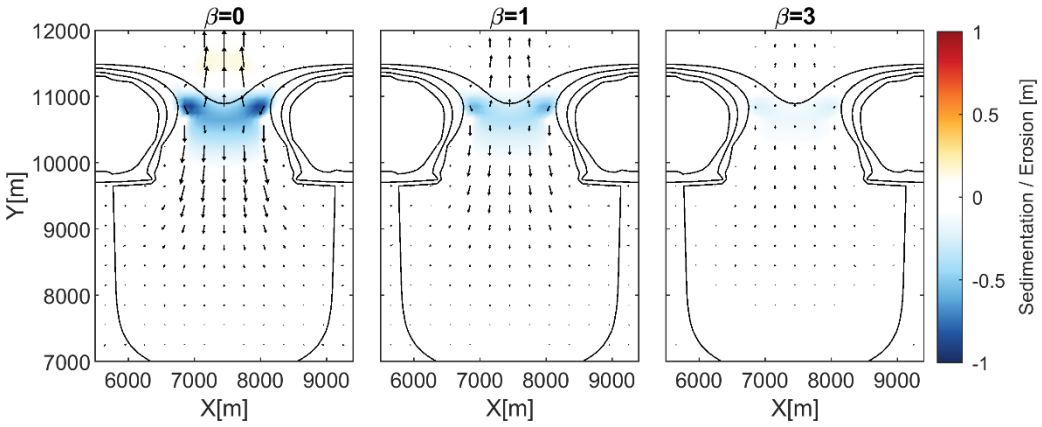

Figure 4.4: Initial morphodynamic response at the inlet with different values for β_m and a homogeneous mud content of 50%. The arrows indicate the residual sediment transport after one tidal cycle.

The increase in resistance of the sand fraction against erosion with increasing values for the mud content that is illustrated by Figure 4.3 and Figure 4.4 corresponds to what was illustrated in Figure 3.1. Especially if the mud content increases, a different value for β_m is going to make a large difference in the resistance against erosion.

4.2.2 Van Ledden

The effect of the two regimes

In the method by Van Ledden, the critical mud content ($p_{m,crit}$) seperates the cohesive regime ($p_m > p_{m,crit}$) from the non-cohesive regime ($p_m < p_{m,crit}$). The effect of these two regimes on the initial morphodynamic response is illustrated in Figure 4.5. For $p_{m,crit}$ = 30% (run 001 in Figure 4.5) the sediment bed is in the cohesive regime, whereas for $p_{m,crit}$ = 40% (run 002) it is in the non-cohesive regime. Note that the initial mud content is the same (35%), the only difference is the defined value for $p_{m,crit}$. Since for these settings the resistance against erosion is slightly higher in the cohesive regime, the erosion in the tidal inlet is smaller in run 001 than in run 002 (see Figure 4.6 for the difference between the two simulations). Consequently, less sediment is (initially) deposited in the ebb- and flood deltas.

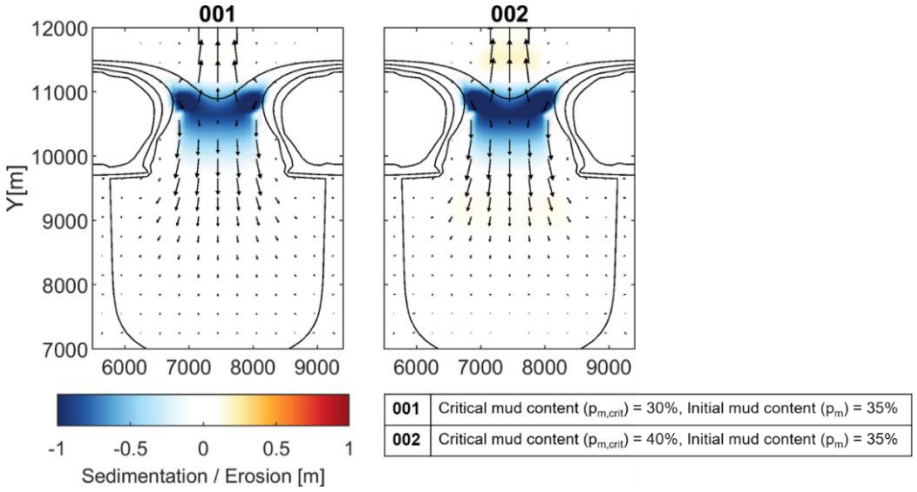

Figure 4.5: Initial morphodynamic response at the inlet for two different combinations of the initial mud content (p_m) and the value set as the critical mud content ($p_{m,crit}$). The arrows indicate the residual sediment transport after one tidal cycle. In these model simulations, β_m was set to 0.

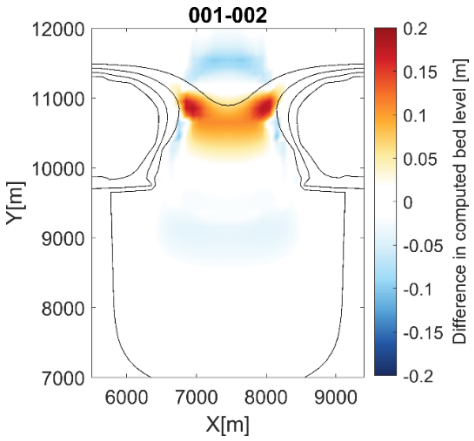

Figure 4.6: Difference in computed bed levels after one tidal period (i.e. the initial morphodynamic response) between runs 001 and 002 (see Figure 4.5). Note that red (blue) indicates more sedimentation (erosion) in run 001 and less erosion (sedimentation) in run 001 than in run 002.

To specify the effect of a shift within the regimes on the erosion of mud, the erosion rate is plotted against the mud content for several values of $p_{m,crit}$ in Figure 4.7. We observe that for a bed shear stress of 2 Pa and a bed with 35% mud, an increase in $p_{m,crit}$ from 30% to 40% (and thus a shift from the cohesive regime to the non-cohesive regime) leads to an increase in mud erosion of about 40%. Comparing the simulations of Figure 4.5, we only see an increase of about 20%, which we relate to the bed shear stresses being different from 2 PA during the simulated period.

The dependence of the erosion of sand on the (cohesive/non-cohesive) regime settings is shown in the right panel of Figure 4.7. Since these erosion rates are directly related to the erosion rates of mud (see also Section 3.2), similar effects are observed.

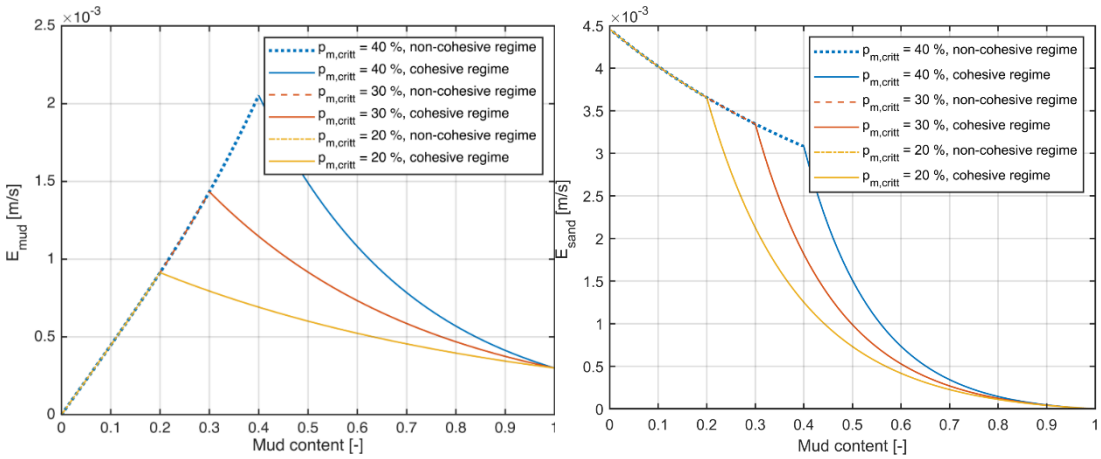

Figure 4.7: Dependence of the erosion of mud (left) and sand (right) on the regime settings according to the Van Ledden formulations. Calculated for τ_b = 2 Pa, $\tau_{e,mud.}$ = 0.5 Pa, $M_e = 10^{-4}$ kg/m^2/s, $D_{50,sand}$ = 150 µm, β_m = 1.

The dependency of the erosion rates on β_m

Figure 4.8 shows the initial morphodynamic response in model simulations in which the sediment bed consists of mainly sand (p_m = 5%). By applying the sand-mud interaction according to Van Ledden (run 002 in Figure 4.8; non-cohesive regime), the initial erosion in the tidal inlet decreased compared to the model simulation without interactions (run 001 in Figure 4.8, see Figure 4.9). In runs 001 and 002, β_m is set to zero. Therefore, the critical bed shear stress for erosion of sand is not affected by the presence of mud. Still, the sediment is considered as a (non-cohesive) mixture. Note that it is possible to include sand-mud interaction by accounting for a cohesive and a non-

cohesive regime, without including the effect of the additional increased critical bed shear stress by setting β_m to zero (run 001).

In runs 003, 004 and 005 in Figure 4.8, the Van Ledden sand-mud interaction is applied together with a value for β_m of 0.75, 1.25 and 3.0, respectively. By increasing β_m, the initial sedimentation and erosion both decrease (see Figure 4.10), which indicates that the seabed becomes more stable for increasing values of β_m. This is similar as observed in the simulations without Van Ledden interaction (see Figure 4.3).

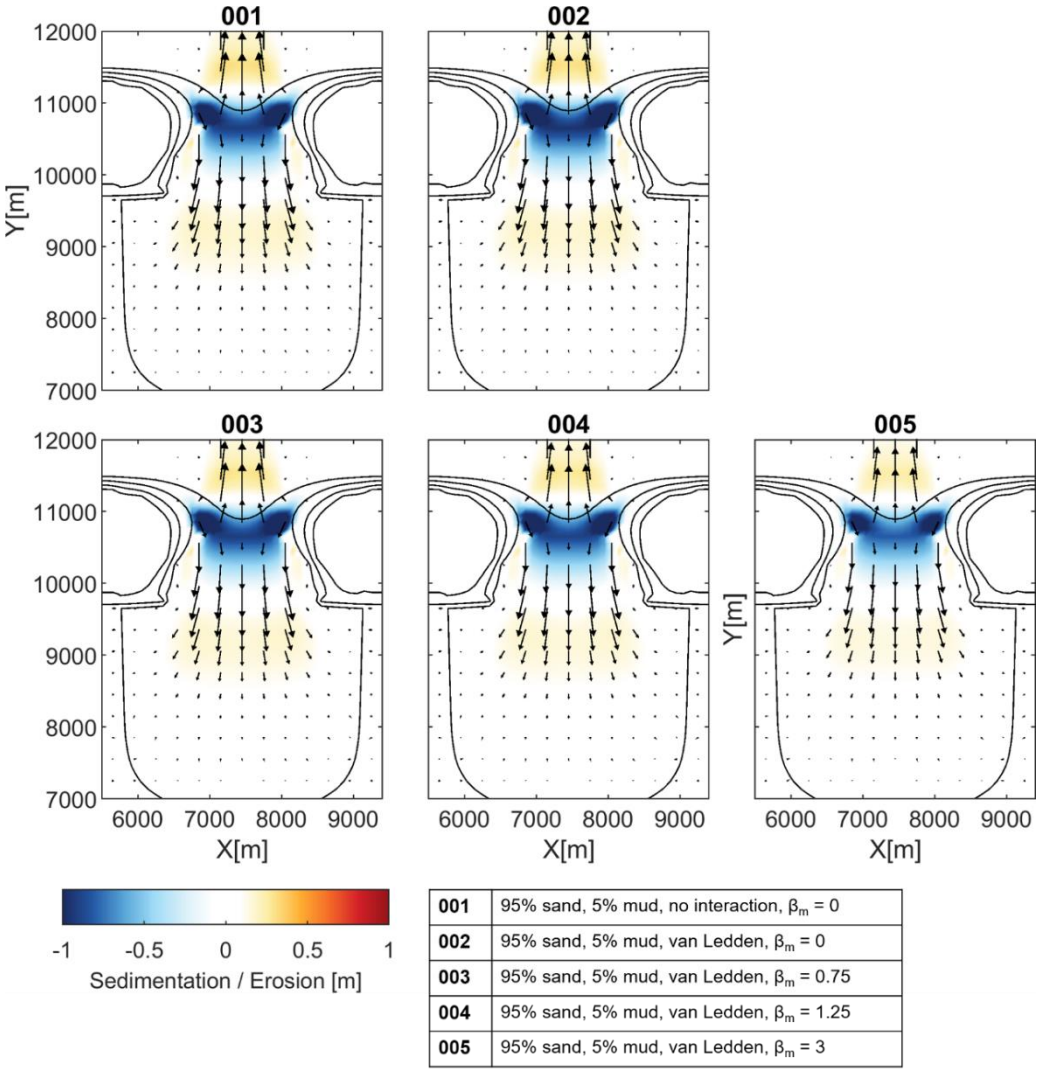

Figure 4.8: Initial morphodynamic response at the inlet for six different sets of settings for the sand-mud interaction. In runs 002 – 005 the critical mud content ($p_{m,crit}$) was set to 30%. The arrows indicate the residual sediment transport after one tidal cycle.

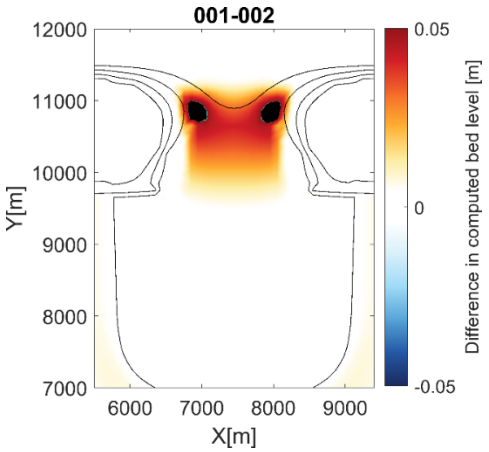

Figure 4.9: Difference in computed bed levels after one tidal period (i.e. the initial morphodynamic response) between runs 001 and 002 (see Figure 4.8). Note that red (blue) indicates more sedimentation (erosion) in run 001 and less erosion (sedimentation) in run 001 than in run 002.

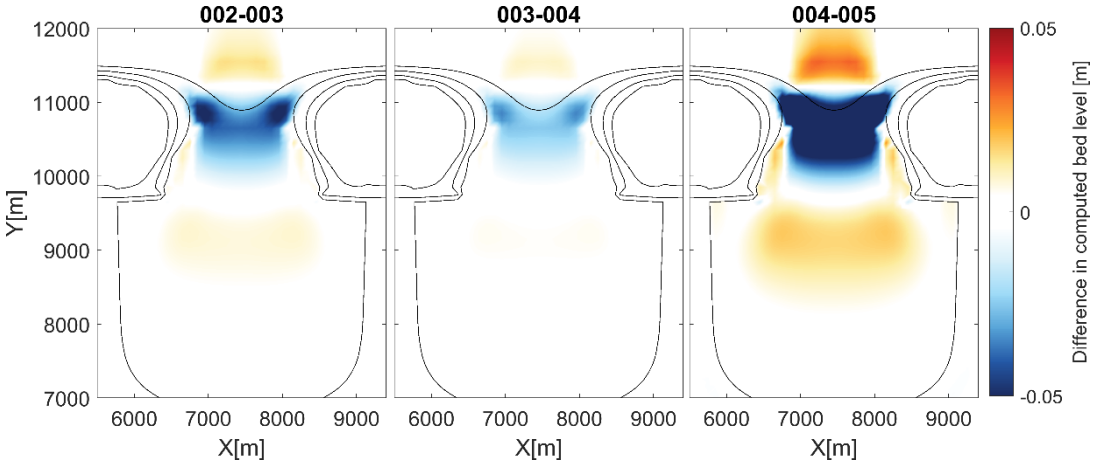

Figure 4.10: Difference in computed bed levels after one tidal period induced by the value of β_m (0.0 in run 002, 0.75 in run 003, 1.25 in run 004 and 3.0 in run 005). Note that red (blue) indicates more sedimentation (erosion) as well as less erosion (sedimentation).

From the aforementioned simulations (Figure 4.8) we conclude that the choice for the value of β_m influences the erodibility of non-cohesive sand-mud mixtures. However, this dependency is also present for cohesive mixtures, since the erosion formulations are set-up such that the erosion rates are the same at the transition between the two regimes. This is also shown in Figure 4.11: the effect of β_m is largest at the transition between the two regimes and becomes 0 for fully (100%) sand/mud sediments.

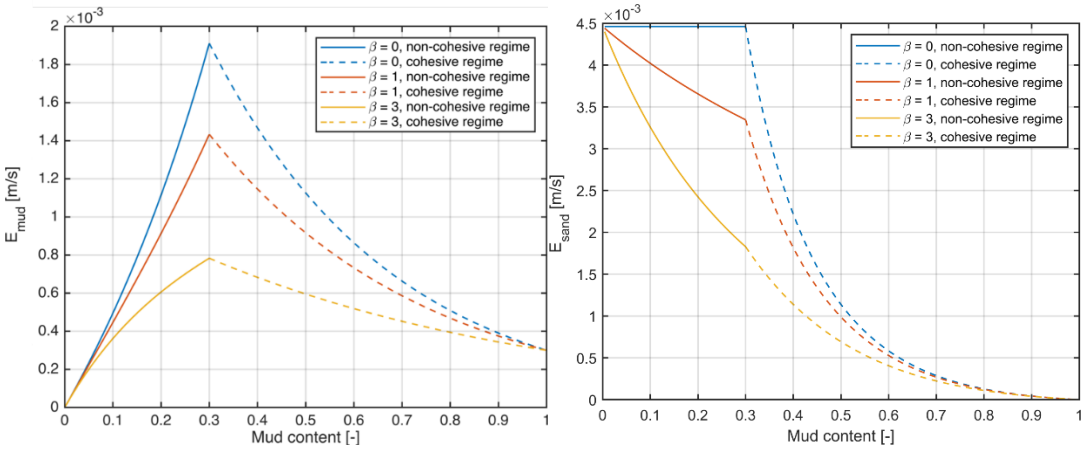

Figure 4.11:Graphical illustration of the dependency of the erosion rate of mud (left) and sand (right) on the mud content for different values of βm. Calculated for τ_b = 2 Pa, $\tau_{e,mud}$ = 0.5 Pa, $M_e = 10^{-4}$ kg/m²/s, $D_{50,sand}$ = 150 μm, $p_{m,crit}$ = 30%.

The dependency of the erosion rates on the settings for the erodibility of mud

The resistance against erosion of the sand-mud mixture is for higher mud contents to a large extent determined by the critical shear stress for erosion of mud ($\tau_{e,mud}$). This is illustrated graphically in Figure 4.12. In the non-cohesive regime, the mixture's critical shear stress against erosion may increase with the mud content if $\beta_m > 0$. In the cohesive regime, the mixture's critical shear stress for erosion is linearly interpolated between $p_m = p_{m,crit}$ and $p_m = 1$ (see Figure 4.12). Whether the mixture's resistance against erosion increases or decreases for higher mud contents in the cohesive regime thus depends on $\tau_{e,mud}$. Figure 4.12 shows that, in case of consolidated mud which is hard to erode (i.e. $\tau_{e,mud} = 0.5$), the critical shear stress for erosion is highest for a mixture with 100% mud. This does imply that in this case the erosion rates of mud will be lowest for pure mud: Figure 4.13 (a) shows that for $\tau_{e,mud} \geq 0.5$, in the cohesive regime, a lower mud content results in more erosion, while in the non-cohesive regime, a lower mud content results in less erosion. Not however, that this is not necessarily the case for unconsolidated mud with low erosion thresholds.

The erodibility of the mud fraction is also influenced by the mobility parameter $M_{e,mud}$. This choice of this parameter value has a similar effect on the mud erosion rates (see Figure 4.13 (b)). In both cases holds that for mobile mud fractions (low $\tau_{e,mud}$, high $M_{e,mud}$) we observe increasing erosion rates with increasing mud content. For mud that is hard to erode (high $\tau_{e,mud}$, low $M_{e,mud}$), we observe maximum erosion rates at the transition between both regimes. The high erosion rates in the non-cohesive regime are caused by the relatively high erosion coefficient for non-cohesive sand-mud mixtures M_{nc}, which is in the order of 10^{-2} for fine sand fractions (100-200 μm). According to Van Ledden (2003) this reflects that mud is easily washed out from the top layer in case of non-cohesive behaviour. This washing out is caused by preferential deposition, i.e. the eroded sand quickly deposits again, whereas the eroded mud stays much longer in suspension. This behaviour was also found in an experimental study by Torfs (1995).

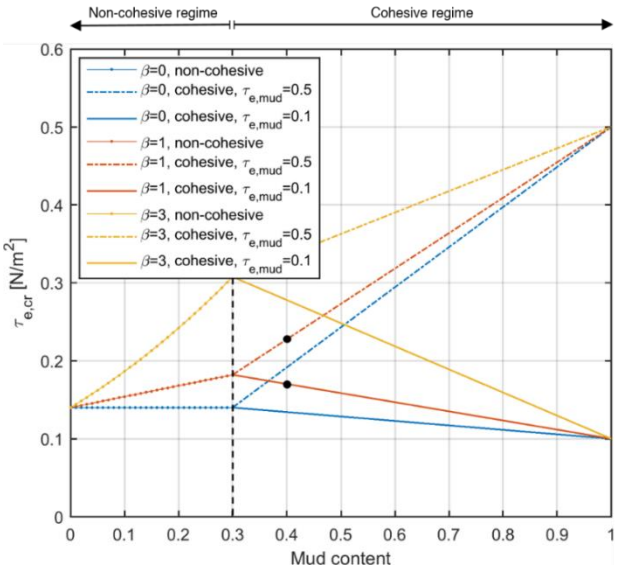

Figure 4.12: Graphical illustration of the dependency of the critical shear stress (of the sand-mud mixture) against erosion on the mud content for different values of β_m and $\tau_{e,mud}$. The black dots indicate the settings of model runs that are discussed in this section.

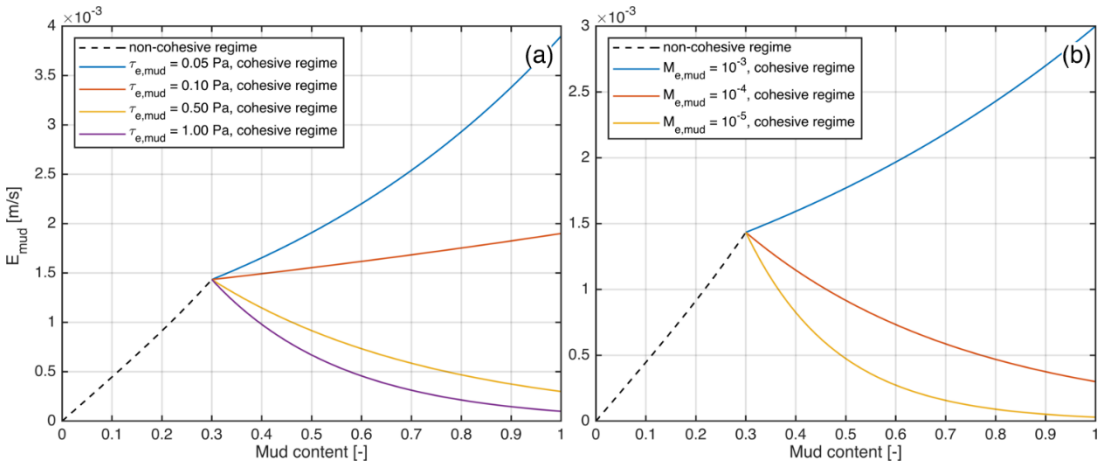

Figure 4.13: Graphical illustration of the dependency of the erosion rate of mud (within the mixture) on the erodibility settings of the mud fraction, with: a) the effect of $\tau_{e,mud}$ and b) of M. Unless stated otherwise, this is calculated for τ_b=2 Pa, $\tau_{e,mud}$ = 0.5 Pa, M_e =10^{-4} kg/m^2/s, $D_{50,sand}$ =150 μm, β_m =1, $p_{m,crit}$ = 30%.

The sensitivity of the initial morphodynamic response to $\tau_{e,mud}$ is illustrated in Figure 4.14. The two evaluated sand-mud interaction settings correspond to the two black dots in Figure 4.12. Again, it is shown that the initial erosion near the inlet decreases for increasing values of $\tau_{e,mud}$, showing a correct implementation of the Van Ledden formulations in Delft3D. This implementation was previously extensively tested by van Kessel, et al. (2012).

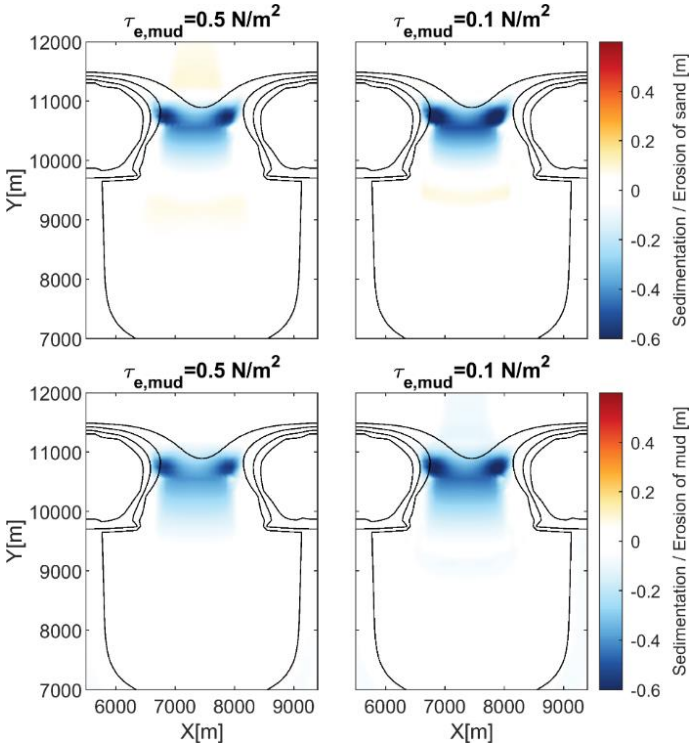

Figure 4.14: Initial morphodynamic response, illustrated as the sedimentation/erosion of sand (top) and mud (bottom), for two different values of the critical shear stress for erosion of mud ($\tau_{e,mud}$). In these model simulations, β_m was set to 0 and $p_{m,crit}$ was set to 0.3.

The dependency of the mud erosion rates on the grain size of the sand fraction

In the non-cohesive regime, mud is eroded proportionally to the erosion of sand. Consequently, mud erosion rates will increase with decreasing D_{50} of the sand fraction. Because of consistency reasons the formulations are such that the cohesive erosion rate and the non-cohesive erosion rates for mud are equal at the transition between both regimes. Therefore, $D_{50,sand}$ also influences E_{mud} in the cohesive regime (see Figure 4.15)

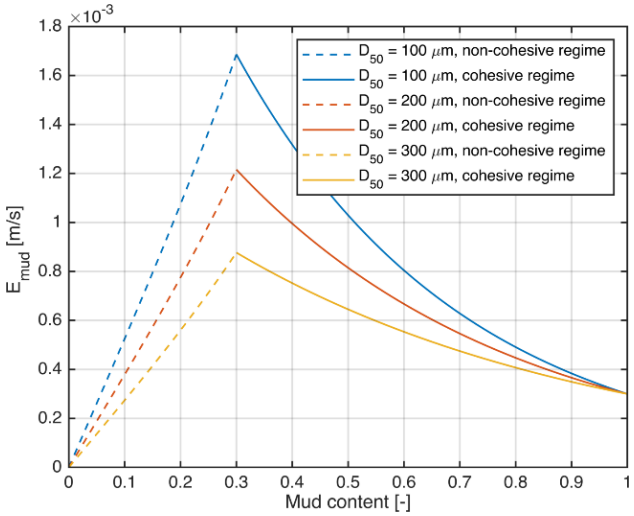

Figure 4.15: Graphical illustration of the dependency of the erosion rate of mud (within the mixture) on the grain size of the sand fraction. Calculated for τ_b = 2 Pa, $\tau_{e,mud}$ = 0.5 Pa, $M_e = 10^{-4}$ kg/m^2/s, $D_{50,sand}$ = 150 μm, β_m = 1, $p_{m,crit}$ = 30%.

4.2.3 Soulsby & Clarke

In the Soulsby & Clarke method, the mud content determines whether *ksSand* or *ksSilt* is used as the roughness height to determine the bed shear stress acting on sediment particles. This was already illustrated in Figure 3.2. Figure 4.16 shows how the bed shear stress on sediment particles changes depending on the mud content for several hydrodynamic conditions (i.e. a combination of a water depth and a current velocity). Whereas the transition zone from *ksSand* to *ksSilt* is symmetric if the roughness height is considered (see Figure 3.2), it is asymmetric if the bed shear stress is considered. This is due to the logarithmic dependency of the bed shear stress on the roughness height. In the example in Figure 4.16, an increase in mud content from 0.3 to 0.4 therefore results in a smaller decrease in the bed shear stress than an increase in mud content from 0.4 to 0.5.

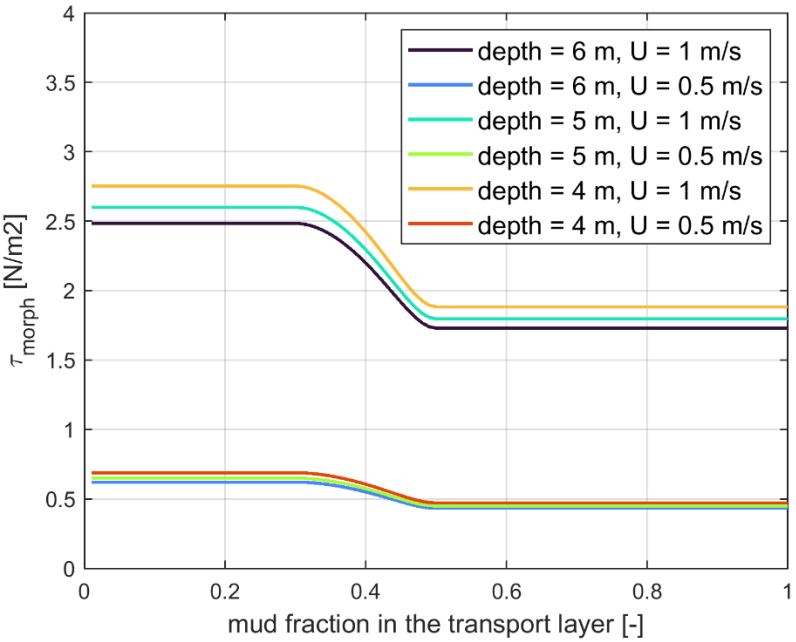

Figure 4.16: Bed shear stress computed by the Soulsby & Clarke method in Delft3D for several hydrodynamic conditions and depending on the mud fraction in the transport layer (i.e. for settings ksSand = 0.02 m, ksSilt = 0.004 m, sc_cmf1 = 0.3 and sc_cmf2 = 0.5 (see Figure 3.2)).

The mud content where the transition between *ksSand* and *ksSilt* takes place may vary per application. In the model simulations that are discussed in this section the initial mud content is constant (at 40%) but the critical transition fraction varies. Figure 4.17 shows the initial morphodynamic response for model simulations in which the transition zone is set from p_m = 20% to p_m = 40% (run 001), from p_m = 30% to p_m = 50% (run 002), and from p_m = 40% to p_m = 60% (run 003). The roughness height *ksSand* = 0.02 m and *ksSilt* = 0.004 m. In run 001 in Figure 4.17, the mud content is higher than the transition zone; *ksSilt* is thus used as the roughness height. In run 003, the mud content is lower than the transition zone and *ksSand* is used. In run 002 the mud content is in the transition zone and the roughness height is determined by an interpolation between *ksSand* and *ksSilt*.

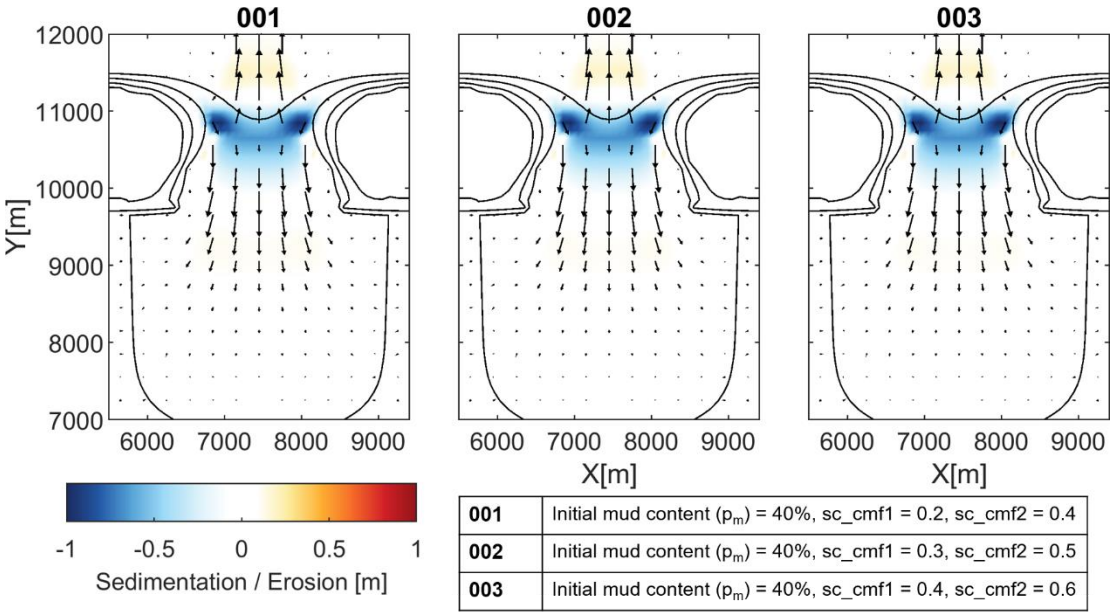

Figure 4.17: Initial morphodynamic response at the inlet for three different simulations with Soulsby & Clarke interaction in which the transition zone between ksSilt and ksSand is at different mud fractions. The initial mud fraction is p_m = 40% in all three simulations.

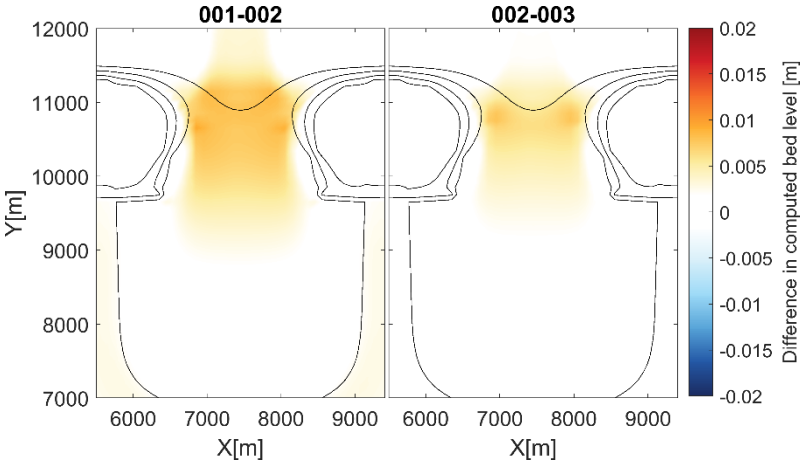

Figure 4.18: Difference in computed bed levels after one tidal period induced by a shift of the transition zone between ksSilt = 0.004 and ksSand = 0.02 (see Figure 4.17).

Because different values for the roughness height are used in the three model runs, the morphodynamic response is different: the bed shear stresses and thus the initial erosion rate are higher if the roughness height increases. This explains why the initial erosion in the tidal inlet in run 002 is higher than in run 001, and higher in run 003 than in run 002 (see Figure 4.18).

By increasing the difference between *ksSand* and *ksSilt*, the effects of the Soulsby & Clarke method become more pronounced, as is illustrated in Figure 4.19 by changing *ksSilt* from 0.004 m (as in Figure 4.18) to 0.001 m.

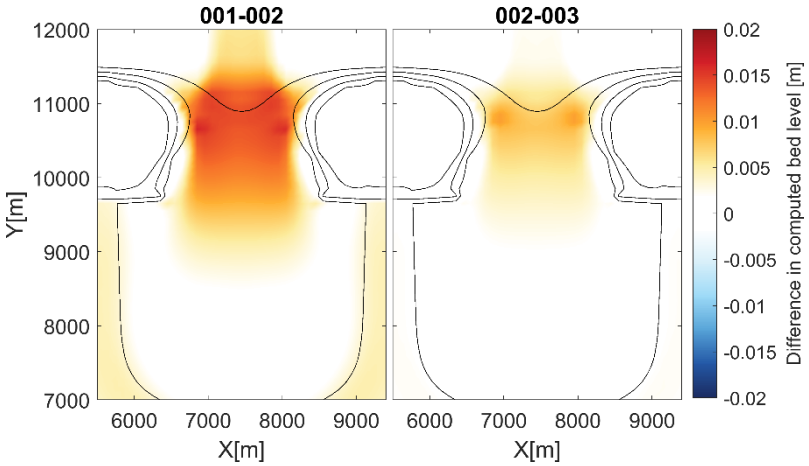

Figure 4.19: Difference in computed bed levels after one tidal period induced by a shift of the transition zone between ksSilt = 0.001 m and ksSand = 0.02 m.

4.3 Long term effects of sand-mud interaction

The effects of sand-mud interaction modules on the long-term morphodynamic development of a tidal basin are investigated by simulating 50 years of morphodynamic development. The initial conditions of this model application have been discussed in Section 4.1.

In discussing the model results, the main focus is on three aspects:

- The morphology after simulating 50 years of morphodynamic development (i.e. pattern of channels and shoals);
- The sediment bed composition after 50 years (i.e. spatial distribution of sand and mud);
- Sand-mud segregation (as introduced in Chapter 2). The sand-mud segregation will often be illustrated by a bimodality in the histogram of the (log-transformed) mud content.

The results will in this chapter be discussed per sand-mud interaction module. For comparison, all figures are also included in Appendix A.2.

4.3.1 Van Rijn formulations

Figure 4.20 shows the bathymetry and the mud fraction in the top layer after simulating 50 years of morphodynamic development with no sand-mud interaction (i.e. β_m = 0). There are two main channels in the tidal inlet. Each of these two channels bifurcate into multiple smaller channels in the tidal basin. A relatively large ebb-tidal delta was formed during the model simulation. This is likely induced by the wave impact at the ebb-tidal delta being relatively low. The mud fraction in the top layer (right part of Figure 4.20) is low in the central part of the basin. Near the closed borders of the basin, the mud fraction approaches 1.

The mud fraction and the log-transformed mud fraction in the top layer are illustrated in histograms in Figure 4.21. The two distinct peaks in the histogram of the mud content are at the two sides of the range; at many places there is either hardly any mud or hardly any sand found in the top layer. The histogram of the log-transformed mud content (i.e. $ln(p_m\ [\%])$, following Herman et al. (2018)) shows the many locations where hardly any sand can be found between log-transformed mud contents of 4 and 5. The peak which indicates locations with hardly any sand is spread over the part with values of the log-transformed mud content lower than 2.

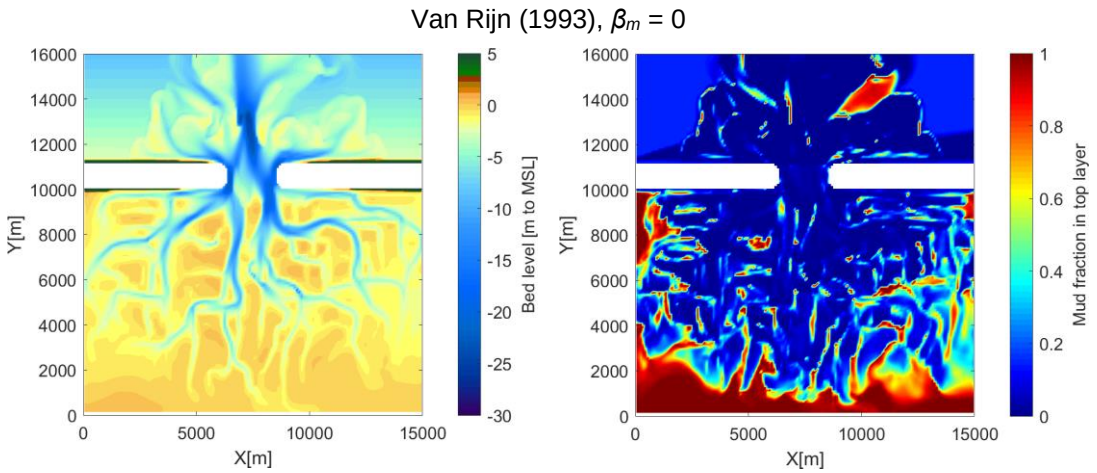

Figure 4.20: Bathymetry (left) and mud fraction in the top layer (by volume, right) after simulating 50 years of morphodynamic development using the Van Rijn (1993) formulations without sand-mud interaction (i.e. β_m=0).

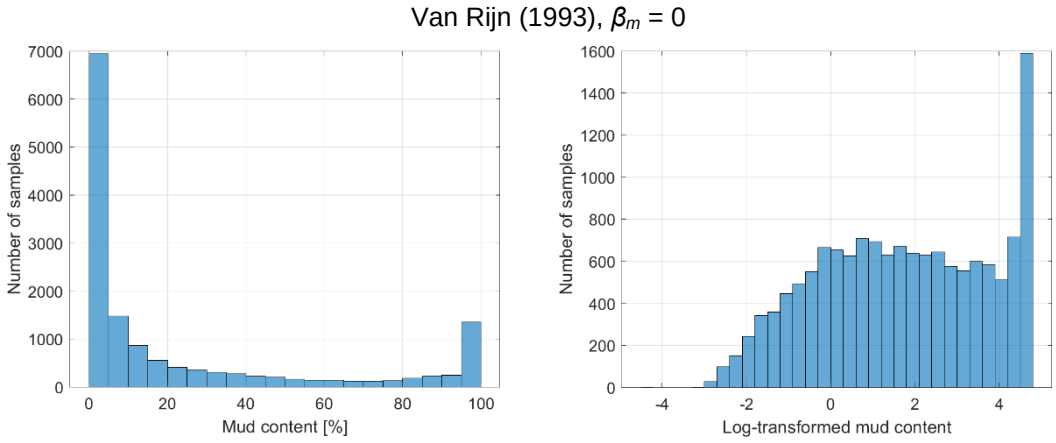

Figure 4.21: Histograms of the mud content (left) and the log-transformed mud content (right, ln(p_m [%])) by mass in the top layer after simulating 50 years of morphodynamic development using the Van Rijn (1993) formulations without sand-mud interaction (i.e. β_m=0). Every grid cell in the tidal basin is used as a sample point in the histograms.

The model simulations without sand-mud interactions (Figure 4.20 and Figure 4.21) will be used as a reference for model simulations with different types of sand-mud interaction in the remaining part of this section. First, the effect of β_m is evaluated. The results of a model simulation with β_m = 1 are illustrated in Figure 4.22 and Figure 4.23. The bathymetry is very different from the results for β_m = 0. One large and two smaller channels are located in the tidal inlet. The mud fraction in the top layer changed accordingly. The histograms particularly show that there are more locations with a high mud content. The second peak in the histogram of the log-transformed mud content (i.e. ln(p_m [%]) ≈ 1.2) has become more distinct. Two peaks in the histogram of the log-transformed mud content is often referred to as bimodality.

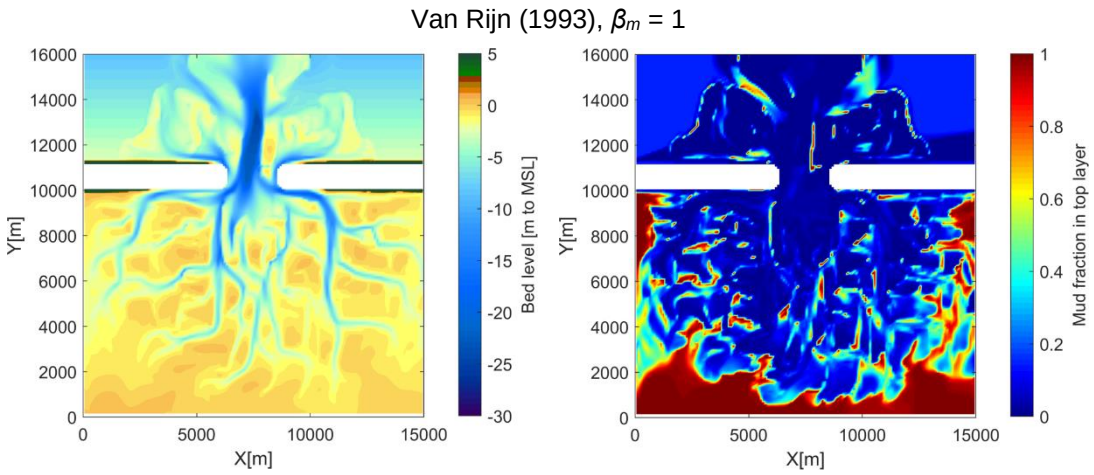

Figure 4.22: Bathymetry (left) and mud fraction in the top layer (by volume, right) after simulating 50 years of morphodynamic development with tide only using the Van Rijn (1993) formulations with β_m = 1.

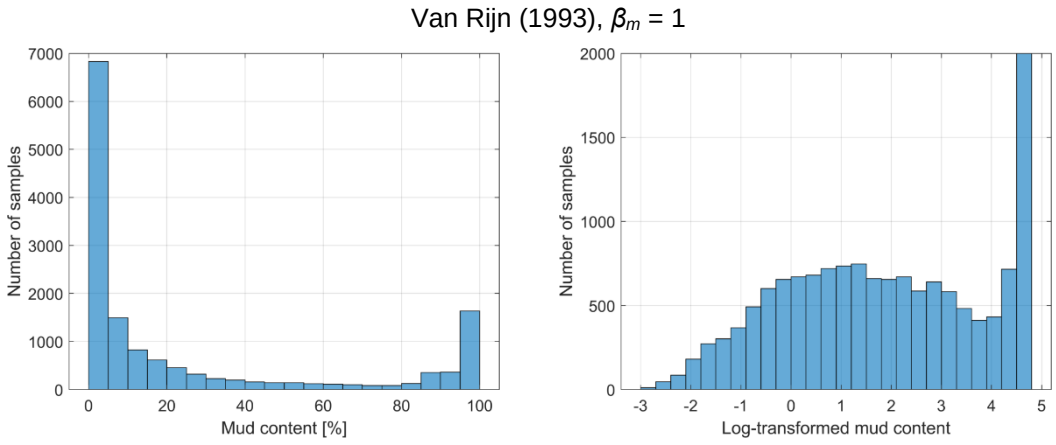

Figure 4.23: Histograms of the mud content (left) and the log-transformed mud content (right, ln(p_m [%])) by mass in the top layer after simulating 50 years of morphodynamic development using the Van Rijn (1993) formulations with β_m = 1.

If β_m is set to 3 instead of 1 (following the original formulation), the morphology again changes considerably. The so-called segregation between sandy and muddy areas becomes more pronounced. The transition zones between sandy and muddy areas have become smaller compared to model simulations that were discussed earlier, such that the gradients in mud content are now larger. This is illustrated in Figure 4.24 and Figure 4.25. In addition, the bimodality in the sediment composition increased. So whereas an increase in β_m mainly limits the erosion of sand in the short term (i.e. as discussed in Section 4.2), it considerably changes the morphology and enhances the segregation of sand and mud in the long term.

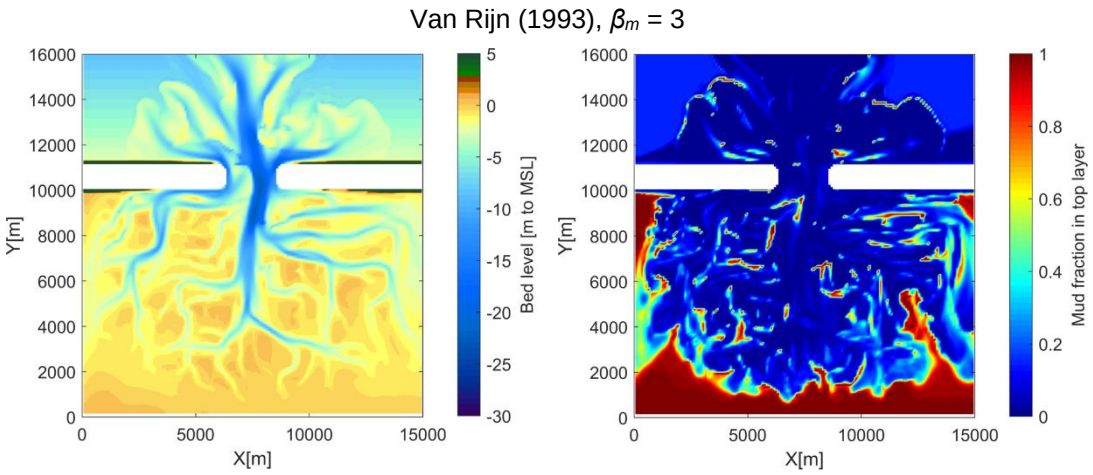

Figure 4.24: Bathymetry (left) and mud fraction in the top layer (by volume, right) after simulating 50 years of morphodynamic development using the Van Rijn (1993) formulations with β_m = 3.

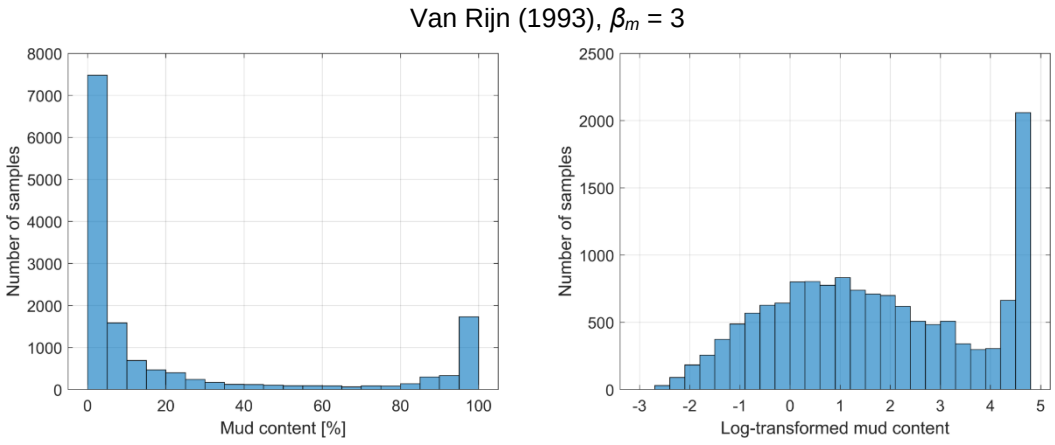

Figure 4.25: Histograms of the mud content (left) and the log-transformed mud content (right, ln(p_m [%])) by mass in the top layer after simulating 50 years of morphodynamic development using the Van Rijn (1993) formulations with β_m = 3.

4.3.2 Van Ledden

In the same manner as for the Van Rijn formulations, 50 years of morphodynamic development has been simulated using the Van Ledden method with β_m = 1. The results are illustrated in Figure 4.26 and Figure 4.27. Compared to model results without Van Ledden interaction (see Figure 4.22 and Figure 4.23), channels propagate less far into the basin. This results in large muddy areas near the borders of the tidal basin. There is a relatively sharp transition from areas with a low mud fraction to areas with a high mud fraction where the basin becomes shallower.

The histograms in Figure 4.27 do not show the bimodality that was the result of model simulations without Van Ledden interaction. The large muddy areas near the borders of the tidal basin are represented in the high peaks on the right of the histograms.

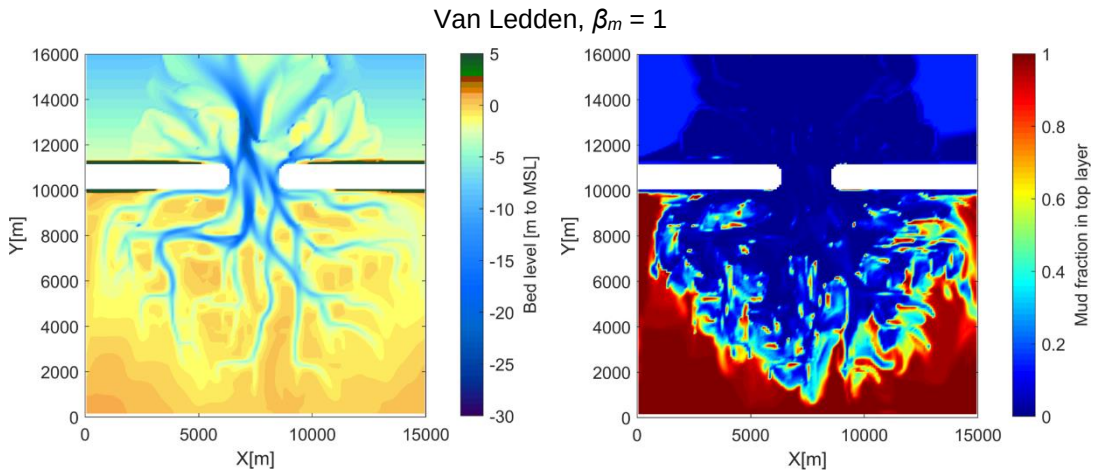

Figure 4.26: Bathymetry (left) and mud fraction in the top layer (by volume, right) after simulating 50 years of morphodynamic development using the Van Ledden method ($p_{m,crit}$ = 0.3) with β_m = 1 in the Van Rijn formulations.

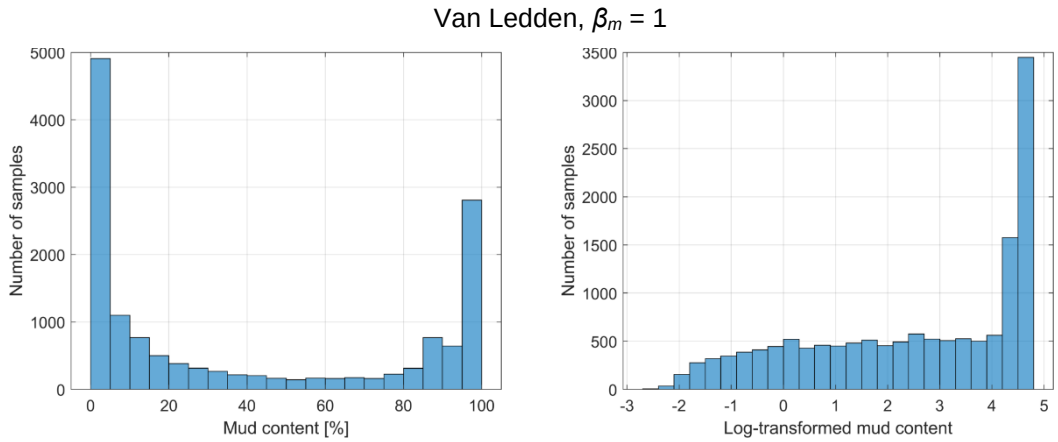

Figure 4.27: Histograms of the mud content (left) and the log-transformed mud content (right, ln(p_m [%])) by mass in the top layer after simulating 50 years of morphodynamic development using the Van Ledden method ($p_{m,crit}$ = 0.3) with β_m = 1 in the Van Rijn transport formulation.

In earlier model runs that are not discussed in this report, using the Van Ledden interaction does lead to an increasing bimodality in the mud content. The main difference between these earlier model runs and the ones presented in this report is that wave conditions were set constant in time. So apparently, it is depending on the wave conditions what the effect of including Van Ledden interaction is on the bimodality in mud content. The results that are presented in this paragraph are thus dependent on the current model settings.

4.3.3 Soulsby & Clarke

The bathymetry and the mud fraction in the top layer by applying the Soulsby & Clarke method with *ksSand* = 0.02 m, *ksSilt* = 0.004 m and a transition zone from *ksSand* to *ksSilt* between mud contents of 30 and 50% is illustrated in Figure 4.28. Note that the combined bed shear stress (i.e. due to currents and waves) is computed differently in case the Soulsby & Clarke method is applied. This causes differences in the forcing conditions compared to the model runs that were discussed earlier, next to the dependency of the bottom roughness on the mud content. However, we also performed simulations with the Soulsby & Clarke method without accounting for sand-mud dependencies of the bottom roughness (by setting *ksSilt* = *ksSand* = 0.02 m), to test whether the results are mainly

influenced by sand-mud interaction or by the different computation of the bed shear stress. These simulations showed that the results that we present here are predominantly steered by the effect of the dependency of the bottom roughness on the mud content.

The tidal channels in Figure 4.28 propagate far into the tidal basins. Between these channels there are relatively shallow areas with patches of high mud content. Generally, the mud content is either high or relatively low: there is only small parts on the edges of the muddy areas where the mud content is between 0.3 and 0.7. This is clearly visible in the histograms of the mud content in Figure 4.29. The histogram of the log-transformed mud content shows the strong bimodality in case the Soulsby & Clarke method is applied.

The influence of the mud content on the bottom roughness in the Soulsby & Clarke method only affects the bed shear stress if the mud content is higher than 30%. Above 30%, the bed roughness starts to decrease, such that the hydrodynamic conditions lead to lower bed shear stresses. Transition zones between channels and tidal flats thus have the tendency to become more muddy once the mud content exceeds 30%. This explains why gradients in mud content have become stronger by applying the Soulsby & Clarke method.

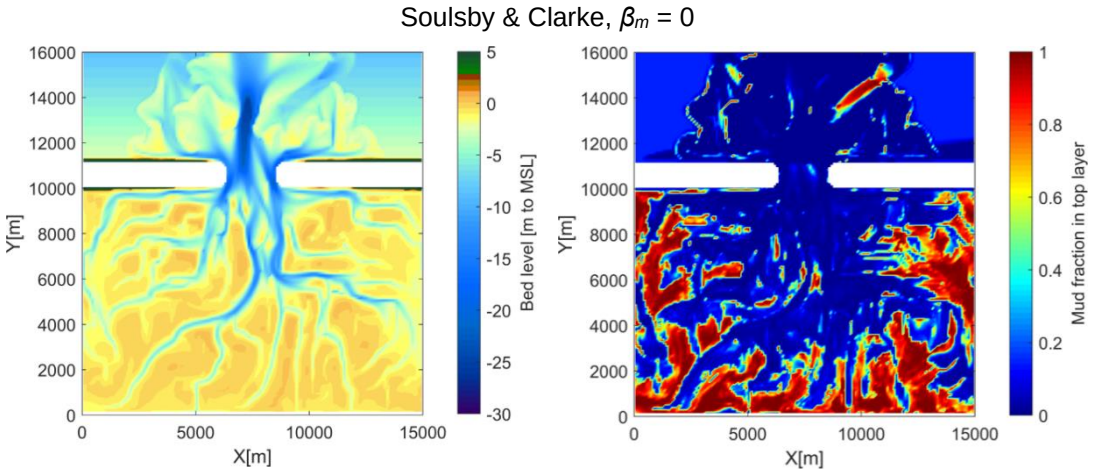

Figure 4.28: Bathymetry (left) and mud fraction in the top layer (by volume, right) after simulating 50 years of morphodynamic development using the Soulsby & Clarke method (ksSand = 0.02 m, ksSilt = 0.004 m) with β_m = 0 in the Van Rijn transport formulation.

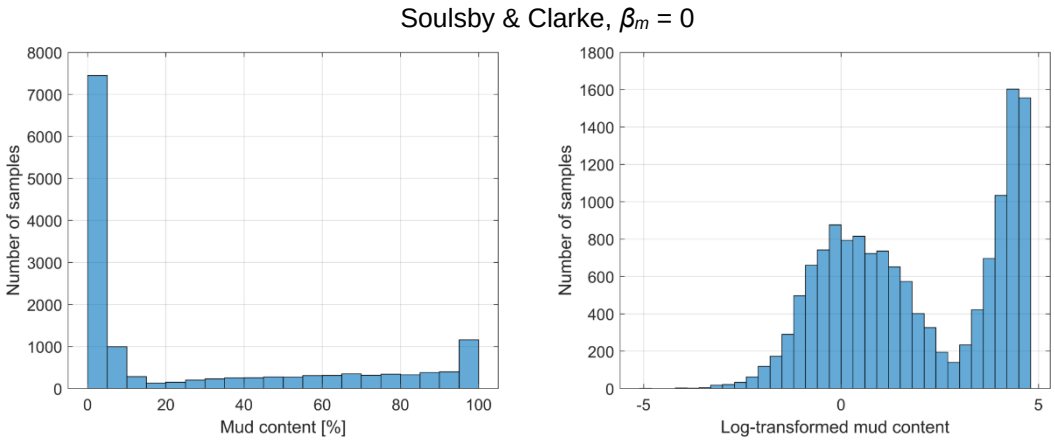

Figure 4.29: Histograms of the mud content (left) and the log-transformed mud content (right, ln(p_m [%])) by mass in the top layer after simulating 50 years of morphodynamic development using the Soulsby & Clarke method (ksSand = 0.02 m, ksSilt = 0.004 m) with β_m = 0 in the Van Rijn transport formulation.

4.3.4 Combined interaction methods

If the different sand-mud interaction methods are combined, the composition of the top layer will affect the critical shear stress for erosion of sand, the erosional behavior of the mixture, and the shear stresses acting on the sediment. The combined effect on the morphology and the mud fraction in the top layer after simulating 50 years of morphodynamic development is illustrated in Figure 4.30 and Figure 4.31. The bathymetry is probably most similar to what was the result of a model run with Van Rijn β_m = 1 (see Figure 4.22), although the channels propagate further into the basin. The spatial variation in mud content is more similar to the results of the Soulsby & Clarke method (see Figure 4.27), because of the distinct edges of muddy areas.

The bimodality in mud content is still visible in the histograms (see Figure 4.31). Due to influences of the other interaction mechanisms, the bimodality is less strong than for only the Soulsby & Clarke method.

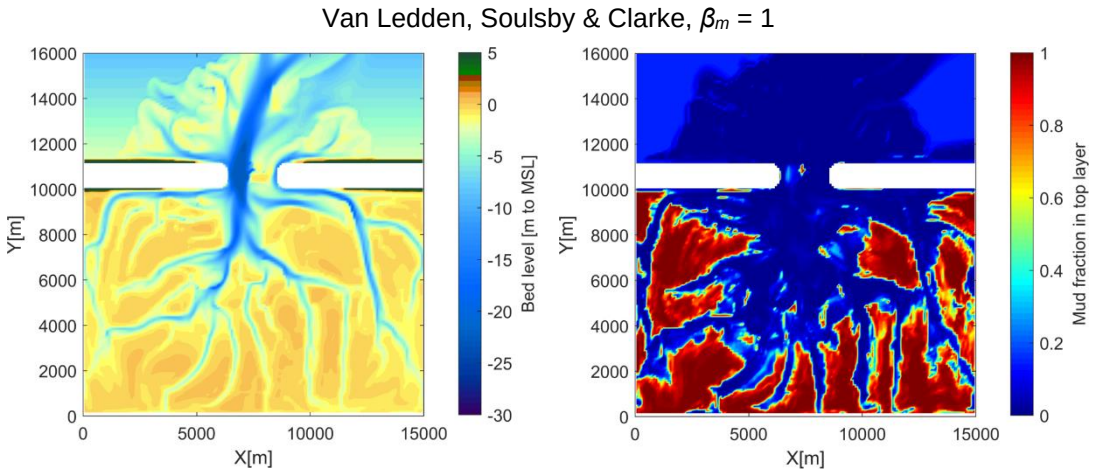

Figure 4.30: Bathymetry (left) and mud fraction in the top layer (by volume, right) after simulating 50 years of morphodynamic development using both the Van Ledden and the Soulsby & Clarke method ($p_{m,crit}$ = 0.3, ksSand = 0.02 m, ksSilt = 0.004 m) with β_m = 1 in the Van Rijn transport formulation.

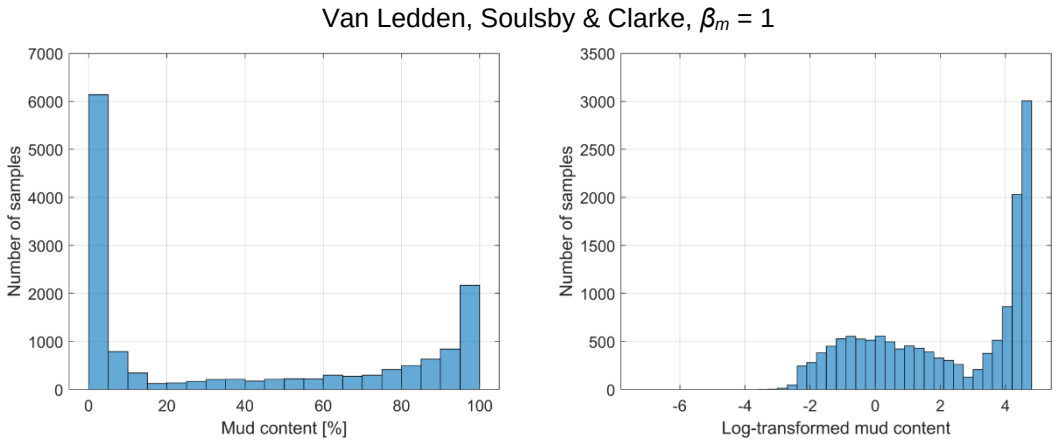

Figure 4.31: Histograms of the mud content (left) and the log-transformed mud content (right, ln(p_m [%])) by mass in the top layer after simulating 50 years of morphodynamic development using both the Van Ledden and the Soulsby & Clarke method ($p_{m,crit}$ = 0.3, ksSand = 0.02 m, ksSilt = 0.004 m) with β_m = 1.

To better understand the effect of combining both sand-mud interaction methods, we have studied how the erosion fluxes are affected when applying both methods simultaneously. From a theoretical point of view, we expect both Soulsby & Clarke (2005) and van Ledden (2003) to reduce the erosion fluxes on mud beds, the former by reducing the bed shear stresses (*load*), and the latter by increasing the critical shear for erosion (*strength*).

Figure 4.32 shows the dependence of the erosion of mud on the mud content, calculated with van Ledden (2003) (orange solid line) accounting for roughness differences and their implications on the bed shear stresses, calculated with Soulsby & Clarke (2005) (blue solid line). This is calculated for a simple test case with currents only, with flow velocities of 1 m/s (panel a) and 0.5 m/s (panel b), and a flow depth of 5 m. For comparison, the dashed lines show what the bed shear stresses and erosion rates would be without accounting for the effect of the mud content on the bed roughness (so calculated with van Ledden, 2003, but without Soulsby & Clarke, 2005). As shown in previous figures, the theory of van Ledden (2003) indeed gives lower erosion fluxes for higher mud contents. As expected, we observe that Soulsby & Clarke (2005) also leads to an important reduction of the mud erosion rates for mud contents above the first critical value (30% in this case). When the bed shear stresses are close to erosion threshold (panel b), the mud erosion fluxes are even reduced to 0.

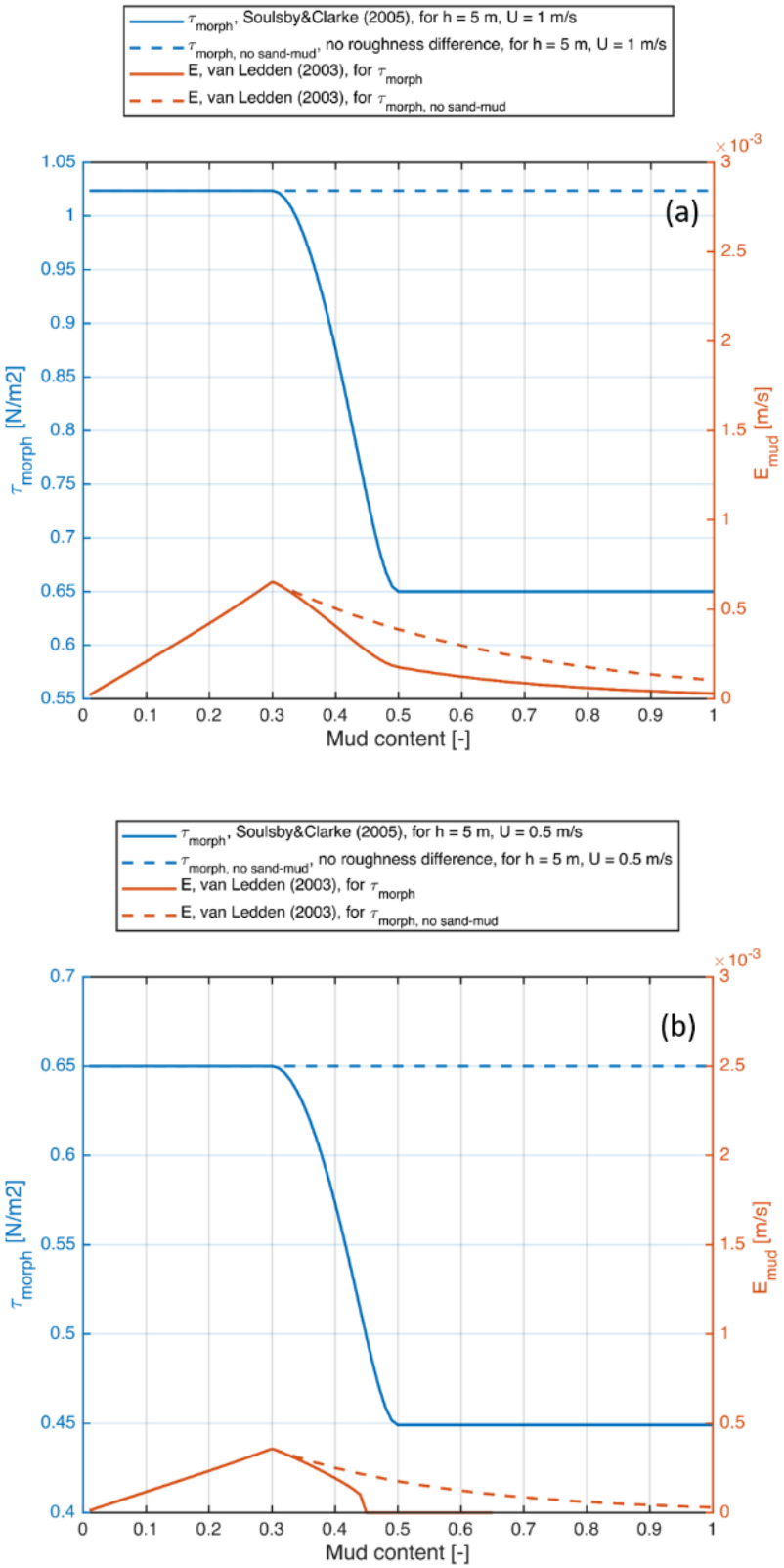

Figure 4.32 Dependence of the bed shear stress and erosion of mud (calculated with van Ledden, 2003) on the mud content. Calculated for $\tau_{e,mud}$ = 0.5 Pa, $M_e = 10^{-4}$ kg/m^2/s, $D_{50,sand}$ = 150 µm, β_m = 1, U=5 m.

4.4 Sensitivity tests for bimodality

4.4.1 Mud availability

To consider the effect of model settings on the results, and more particularly on the bimodality of the mud content, several model runs with adjustments to the original settings were performed. The first adjustments are related to the availability of mud in the system. This is done by (1a) increasing the initial mud content from 5% to 10%, by (1b) lowering the initial mud content to 2% and by (2) increasing the concentration of mud at the model boundary from 5 mg/l to 50 mg/l. The model run with all three different sand-mud interaction mechanisms is used as a reference for these adjustments.

Changing the mud content in the initial sediment bed

In case the initial mud content increases, the mud content in the system after 50 years of morphodynamic simulation increases accordingly. In a similar manner, the mud content decreases if the initial mud content decreases. This is illustrated in Figure 4.33. Due to changes in the initial mud content, the ratio between the two peaks in the histograms of the bimodality changes. This is illustrated in Figure 4.34. The results show that with increasing mud availability, the right peak of the bimodality becomes larger, meaning that more sites become muddy. Vice versa, the left peak becomes larger (more sites becoming sandy) with decreasing mud content. However, in all cases the bimodality remains, and a strong sand-mud segregation is observed in all cases.

Not only the sediment composition is affected with increasing mud content, but also the bathymetry (as shown in Figure 4.35). In general, tidal flats become larger and higher with increasing mud availability.

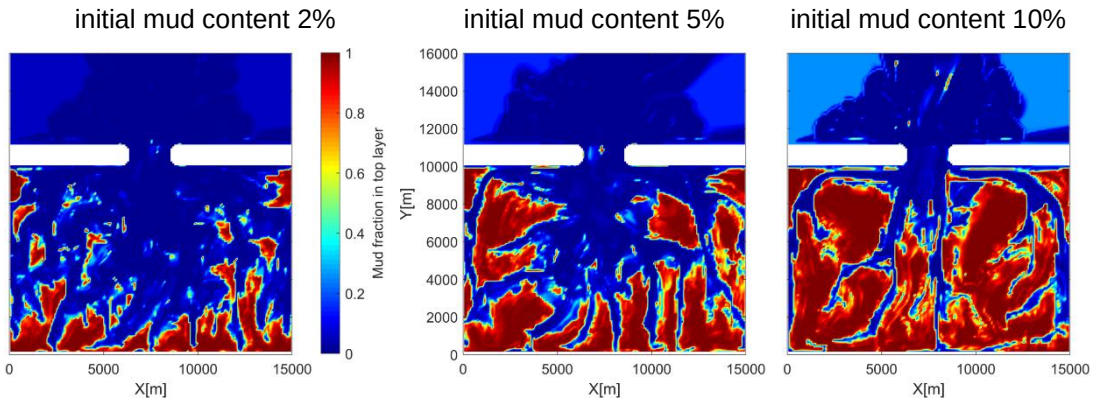

Figure 4.33: Mud fraction in the top layer (by volume) after simulating 50 years of morphodynamic development using both the Van Ledden and the Soulsby & Clarke method ($p_{m,crit}$ = 0.3, ksSand = 0.02 m, ksSilt = 0.004 m) with β_m = 1 in the Van Rijn transport formulation for three model runs with different initial mud content.

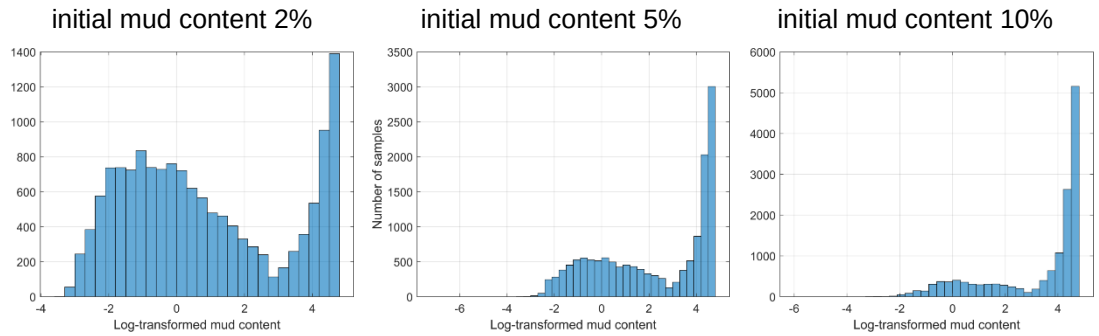

Figure 4.34: Histograms of the log-transformed mud content (ln(p_m [%])) in the top layer after simulating 50 years of morphodynamic development using both the Van Ledden and the Soulsby & Clarke method ($p_{m,crit}$ = 0.3, ksSand = 0.02 m, ksSilt = 0.004 m) with β_m = 1 for three model runs with different initial mud content. Please note the axes differ.

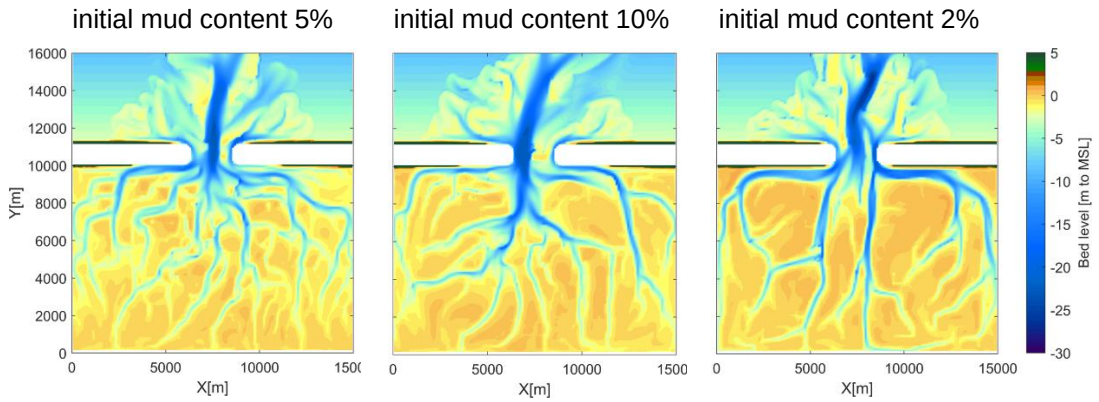

Figure 4.35 Bathymetry after simulating 50 years of morphodynamic development using both the Van Ledden and the Soulsby & Clarke method (pm,crit = 0.3, ksSand = 0.02 m, ksSilt = 0.004 m) with β_m = 1 in the Van Rijn transport formulation for three model runs with different initial mud content.

Changing the mud concentration at the model boundary

If the mud concentration at the model boundary increases, the mud content in the bed after 50 years of morphodynamic development increases. This is illustrated in Figure 4.36. The increase in the availability of mud has a similar effect on the bimodality in the system as increasing the initial mud content (see Figure 4.37); the peak related to high mud contents increases in size, whereas the peak related to low mud contents decreases.

Again, we observe that tidal flats are larger and especially higher with increasing mud availability (Figure 4.38)

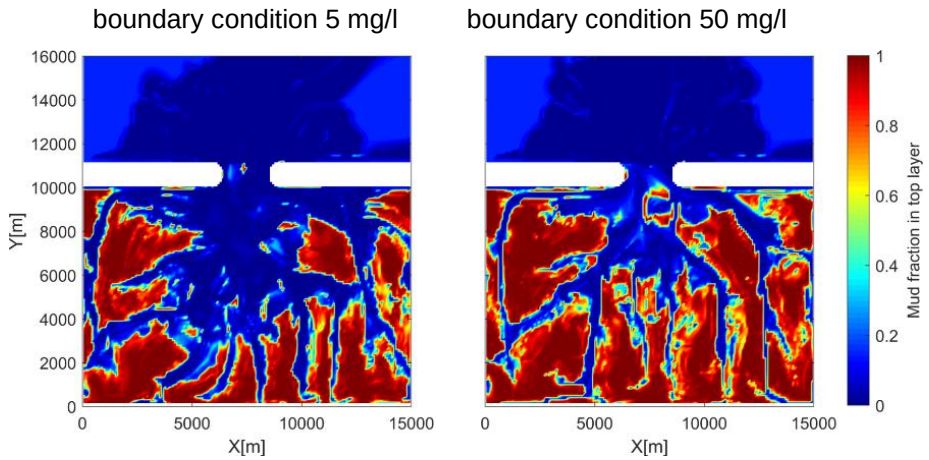

Figure 4.36: Mud fraction in the top layer (by volume) after simulating 50 years of morphodynamic development using both the Van Ledden and the Soulsby & Clarke method ($p_{m,crit}$ = 0.3, ksSand = 0.02 m, ksSilt = 0.004 m) with β_m = 1 in the Van Rijn transport formulation for two model runs with different mud concentrations at the model boundary.

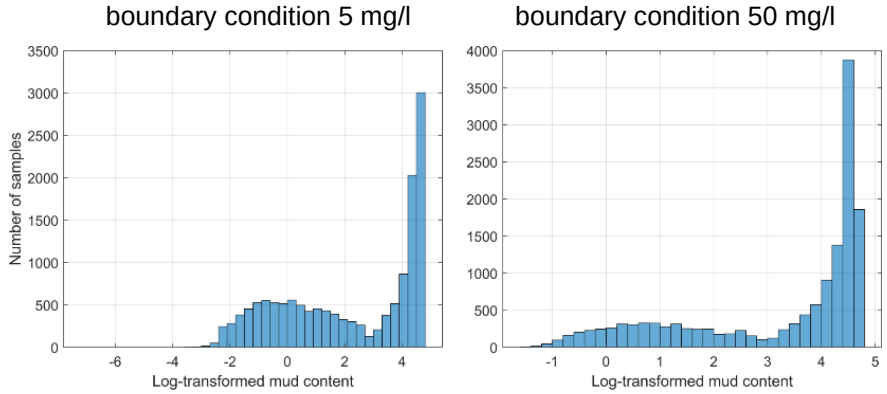

Figure 4.37: Histograms of the log-transformed mud content (ln(p_m [%])) in the top layer after simulating 50 years of morphodynamic development using both the Van Ledden and the Soulsby & Clarke method ($p_{m,crit}$ = 0.3, ksSand = 0.02 m, ksSilt = 0.004 m) with β_m = 1 for two model runs with different mud concentrations at the model boundary. Please note the axes of the two plots differ.

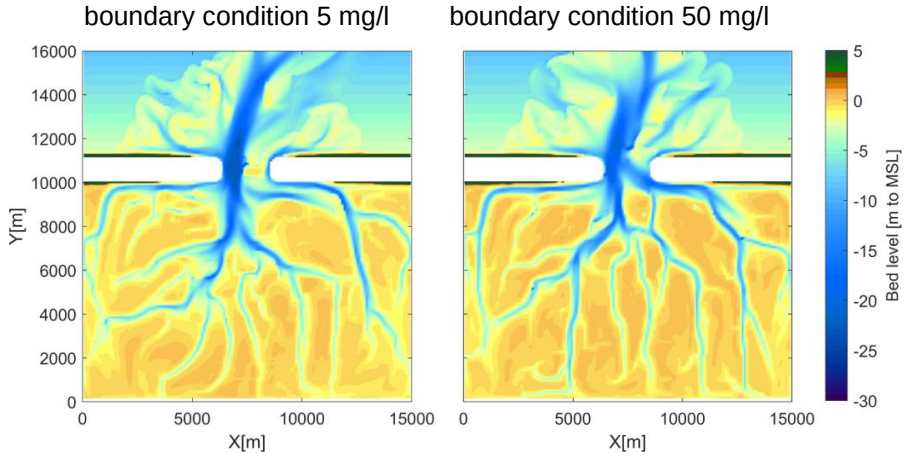

Figure 4.38 Bathymetry simulating 50 years of morphodynamic development using both the Van Ledden and the Soulsby & Clarke method (pm,crit = 0.3, ksSand = 0.02 m, ksSilt = 0.004 m) with β_m = 1 in the Van Rijn transport formulation for two model runs with different mud concentrations at the model boundary.

4.4.2 Regime thresholds

The results of Section 4.3.3 show that accounting for the changes in bed roughness depending on the mud content does enhance the bimodal distribution of the mud availability in the sediment bed. To test the dependency of this distribution on the (user defined) transitions between the regimes, the simulations with different transitions are compared. The transition determines the mud content at which ksSilt is used for the computation of the bed roughness (instead of ksSand), see also Section 3.3. The values of ksSilt and ksSand remain the same for both simulations (0.004 and 0.02 respectively).

Figure 4.39 shows the resulting sediment composition for both simulations after 50 years. The general patterns do not differ much. However, if we compare the statistical distributions of both results (see Figure 4.40), a trend becomes visible: by shifting the transition zone towards a higher mud content, the dip in between the two peaks, which represents the mud-content that occurs the least, also shifts towards a higher mud content (around the new transition zone). In fact, not only the dip is shifted, but also the left peak, which can be interpreted as that the areas with a low mud content become slightly muddier.

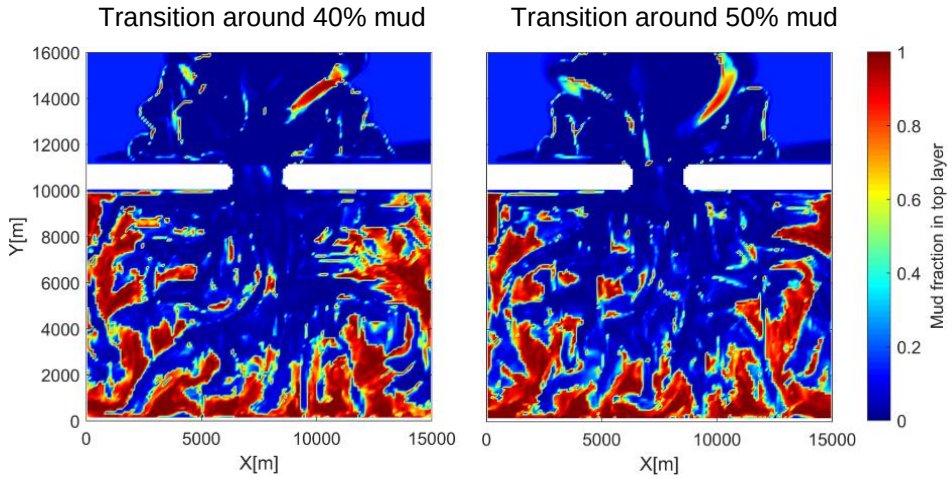

Figure 4.39 Mud fraction in the top layer (by volume) after simulating 50 years of morphodynamic development using the Soulsby & Clarke method (ksSand = 0.02 m, ksSilt = 0.004 m, with β_m = 0) with different values for the transition for using ksSilt as the roughness height.

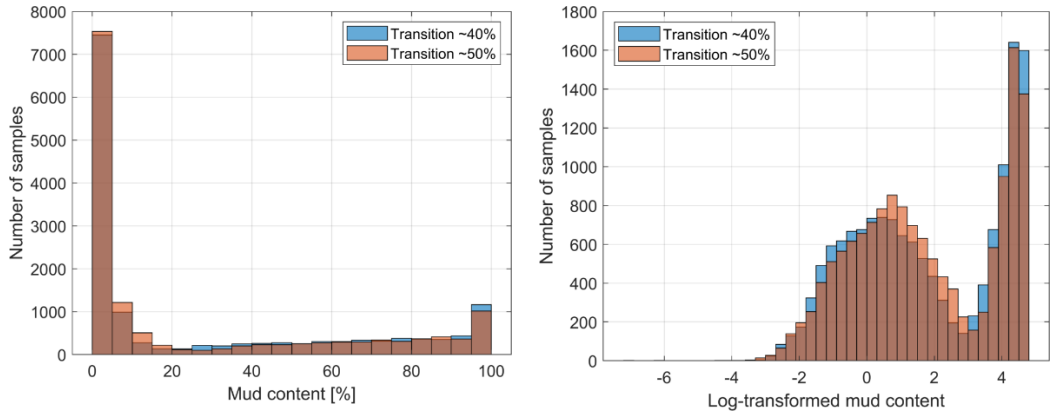

Figure 4.40 Histograms of the mud fraction in the top layer (by mass, left: prior to log-transformation, right: after log- transformation) after simulating 50 years of morphodynamic development using the Soulsby & Clarke method (ksSand = 0.02 m, ksSilt = 0.004 m, with β_m = 0) with different values for the transition for using ksSilt as the roughness height.

5 Discussion

User defined parameters Van Ledden

When applying the theory of Van Ledden in a morphodynamic calculation, there is only one parameter to be defined by the user, which is the critical mud content that defines the transition from non-cohesive to cohesive behavior ($p_{m,crit}$). Van Ledden states that the cohesive behavior of a mixture is defined by the clay content, and that the transition takes place at a clay content between 5 -10%, depending on the type of clay. Since Dutch tidal basins and estuaries have an approximately constant clay/silt ratio (varying within a narrow range between 0.16 and 0.25), the critical clay content can be translated into a critical mud content. In practice, often the choice is made for $p_{m,crit}$ = 0.3, following the example of the Western Scheldt by Van Ledden et al. (2004) (here the authors assumed a critical mud content of 7.5% and a clay/silt ratio of 0.25. However, one should keep in mind that $p_{m,crit}$ will differ for systems with a different clay/silt ratio, or for systems with a different type of clay (5 -10% clay corresponds to 20-40% mud in case of clay/silt = 0.25). This parameter choice will have a noticeable impact on the predicted erosion rates, especially for beds with a mud content around the critical value (see Figure 4.7).

By default, β_m is set to 3 when using the Van Rijn formulations in Delft3D. Note however, that this would lead to a significant increase (and possibly overestimation) of the bed strength against erosion when combined with Van Ledden sand-mud interaction (Figure 4.11 shows erosion rates would decrease up to 40% when setting β_m to 3 instead of 1). According to Van Ledden (2003), this coefficient should be set at 0.75-1.25, and may depend on the packing of the sediment. Further research is needed to determine this dependency. However, our results show that the sensitivity for β_m within the given range is much smaller than the sensitivity for $p_{m,\,crit}$.

Although the critical erosion threshold of mud is not a user defined parameter of the Van Ledden formulations only (it is a rather general sediment parameter), it is important to note its influence on the outcome of the erosion formulations. Whereas high critical values ($\tau_{e,mud}$ = 0.5-1 Pa, representing mud that is (partly) consolidated and hard to erode) will result in maximum erosion rates at $p_m = p_{m,\,crit}$, for lower values ($\tau_{e,mud}$ < 0.1, indicating fresh mud deposits) we observe an increase in erosion for an increasing mud content of the bed. The same holds for the erosion parameter M. It is not clear whether Van Ledden (2003) intended this behaviour, since he states that*: "For natural muds, the critical erosion shear stress varies between 0.1 and 0.5 N/m^2."* Besides, all of his applications involve low values of *M* and relatively high values of $\tau_{e,mud}$.

User defined parameters Soulsby & Clarke

To investigate the effects of the Soulsby & Clarke method in morphodynamic computations, the user defined settings for the roughness height of the sediment bed were set to *ksSand* = 0.02 m and *ksSilt* = 0.004 m. These values were chosen based on earlier experiences in modelling either sandy or muddy systems. With typical values for the water depth and the flow velocity in a tidal system, the flow would always be considered as a rough turbulent flow as long as *ksSilt* = 0.004 m. The flow over freshly deposited mud beds may however be hydrodynamically smooth (Soulsby & Clarke, 2005). This part of the parameter space of the Soulsby & Clarke method in Delft3D has not been considered in this study, since the difference between *ksSand* and *ksSilt* was relatively small in all applications. By increasing the difference between *ksSand* en *ksSilt* - and in particular by decreasing *ksSilt* such that the flow becomes hydrodynamically smooth - the effect of the Soulsby & Clarke may be more pronounced.

The transition zone in the roughness height between *ksSand* and *ksSilt* was in this study often set between mud fractions of p_m = 0.3 and p_m = 0.5. In this way, the roughness height is the same in all areas with little mud ($p_m \leq 0.3$). Similarly, the roughness height is the same in all muddy areas (p_m

≥ 0.5). These settings more or less impose the bimodality in the mud content, since sandy areas will not become muddy as long as a slight increase in the mud content does not affect the roughness height. At the moment, it is not really clear what would physically be the right width of the transition zone. If for example the transition zone is set between p_m = 0.1 and p_m = 0.9, every small adjustment to the bed composition within this range would yield a different roughness height in the next timestep. It would then be easier for a sandy area to become muddy, and vice versa.

Application of sand-mud interaction in morphodynamic modelling

In long-term simulations with calm conditions and low mud contents, the effect of including sand-mud interaction might seem small at first sight (slight reduction/increase of erosion rates). However, as showed in the results, including sand-mud interaction (i.e. either by the formulations of Van Rijn, Van Ledden or Soulsby & Clarke) leads to more sharp transitions between the predominantly sandy areas (often the channels) and the muddy areas on top of the flats. These transitions have often been observed in the field (Van Straaten & Kuenen, 1957; de Glopper, 1967; Zwarts, 2004; Van Ledden, Sand-mud segregation in estuaries and tidal basins, 2003). Apparently, we need to account for these interaction mechanisms in morphodynamic models in order to reproduce the sharp gradients.

The sand-mud interaction mechanisms are expected to be important in studies with a large scale and long-term perspective, since the interaction between channels and shoals is then very relevant. In long-term studies in which shoal growth or decay plays a role (e.g. adaptation to SLR), the interface between channels and shoals must be reproduced correctly in morphodynamic models in order to investigate the supply of sediment towards intertidal shoals. In particular, the growth of these intertidal shoals is relevant for the adaptation of shallow tidal systems to SLR.

In short-term simulations, including sand-mud interaction may have a significant impact on the calculated erosion rates. Depending on the application in a study it may therefore be necessary to include the sand-mud interaction mechanisms in a morphodynamic model. One could, for example, think of a study site where the supply of sediment is stirred by local erosion of a sand-mud mixture. Reproducing the erosion rate of the mixture correctly would then be necessary in order to assess both the short-term morphodynamic response in the system and the effect of erosion on concentrations of suspended matter. Since erosion will act as a source of sediment for concentrations in the water column, reproducing the erosion rates correctly is of large importance for modelling mud dynamics (i.e. concentrations and transport).

Drivers for a bimodal distribution of the mud content in the sediment bed

There are both physical and ecological processes that may promote positive feedbacks, resulting in the observed bimodal distribution of the mud content. In this report we have showed the potential effect of physical drivers. It was found that including the variability of the bed roughness depending on the sediment composition (using the method by Soulsby&Clarke) strongly enhances the bimodality, generating sharp spatial transitions between the sandy and muddy areas. Increasing the critical bed shear stress for erosion of sand with increasing mud content (by increasing the parameter β_m from 0 to 3) also has this effect although much less pronounced. Implementing sand-mud interaction based on the theory of van Ledden (2003) showed inconsistent results with respect on the bimodal distribution, depending on the modelling approach. It was found that for some modelling settings (e.g. using a Chézy value for the bed roughness, or calculating the waves with one single average wave condition) the model predicted a strong bimodality, while for other settings (such as the ones showed in Section 4.3.2) the bimodality remained absent. Further research will be needed to understand the cause.

Ecological processes that may enhance the bimodality have been studied in previous researches. Grabowski, et al. (2011) review evidence that microphytobenthos EPS can substantially increase the critical shear stress for erosion and reduce erosion rates. Van de Koppel, et al. (2001) combined

this with the observation that the biomass of microphytobenthos tends to be higher in muddy than sandy sediments to generate a model predicting bimodality of mud content in sediments.

Synthesis

Various previous studies (e.g. Van Ledden (2003); Winterwerp & Van Kesteren (2004); Jacobs (2011)) have showed the considerable effect of sand-mud interaction on morphodynamics based on laboratory and field experiments, and modelling studies. In this study we have shown the effects of accounting for sand-mud on the morphodynamic predictions of Delft3D. Remarkable effects were observed on both the bed level evolution and the bed sediment composition. This can improve modelling studies with:

1. An ecological perspective: Since sediment composition largely influences biota (and vice versa), and now a realistic sand-mud segregation can be reproduced.
2. A long-term perspective (such as sea level rise related research): we have shown that accounting for sand-mud interaction influences long-term prediction, including general parameters such as the bimodality of the mud content and the relation between the mud content and the bed shear stress.
3. A short-term perspective with respect to local sedimentation and erosion (such as channel maintenance studies). It was shown that sand-mud interaction can largely alter sedimentation rates.

Below an overview of the functionality of the modules is provided:

- Van Rijn (1984, 1993, 2007), β_m

  What it represents: An increased value of β_m is used to simulate the effect of an increased threshold for erodibility of sand when the mud content increases. This does not affect the erosion rates of mud. Sand and mud transport are calculated separately (e.g. with the formulations of van Rijn and Partheniades-Krone respectively).

  Effects on model results: For sand-mud mixtures with high mud content, transport rates are largely reduced when increasing β_m. In long-term prediction, this enhances sharp transitions between muddy and sandy areas.

  Notes and pitfalls: When β_m is set to 0, the mud content will not influence the erodibility of sand. Note that β_m is automatically set to 3 in Delft3D. This should be changed to 0.75-1.25 when combined with van Ledden (2003).

- Van Ledden (2003)

  What it represents: Sand-mud mixtures can be either non-cohesive or cohesive depending on the clay content (which can be expressed as the mud content). The erosional behavior is significantly different for the two regimes and within the regimes, sand and mud erosion are interdependent. For non-cohesive sand-mud mixtures ($p_m < p_{m,cr}$), mud is eroded proportionally with sand instead of being eroded individually. The bed becomes cohesive when the mud content in the bed exceeds the critical mud content. The erosive behaviour of such mixtures takes place as suspended transport only and the erosion of the sand-particles is proportional to the erosion of mud.

  Effects on model results: For muddy sediments that are hard to erode (τ_e =0.5-1.0 Pa) maximum erosion rates of mud will occur when the mud content is close to the critical mud content. This increases sand-mud segregation and enhances sharp transitions between sandy and muddy areas.

  Notes and pitfalls: This module was set-up and implemented in combination with the van Rijn formulations for sand transport, and it cannot be used properly with other formulations, such as Engelund-Hansen (1967) (as showed by Braat et al, 2017). Note that for the

formulations of van Rijn, β_m is automatically set to 3. According to van Ledden (2003) 0.75-1.25 is a better choice, since this gives a better representation of the critical bed shear stress for erosion of sand in the non-cohesive regime (and in the cohesive regime, sand is eroded proportionally with mud). Note that the transition between the regimes takes place at a user-defined critical mud content (which should be derived from the critical clay content, 5-10%, and the local clay/silt ratio). This transition is implemented as a gradual transition with regard to the erosion flux E, which does not have a discontinuity at the critical mud content $p_{m,crit}$

- Soulsby & Clarke (2005)
  What it represents: When using the method of Soulsby & Clarke (2005) to calculate the bed shear-stress generated by waves and currents, the bed roughness is calculated with either the roughness height of sand or mud (ksSand and ksSilt), depending on the mud content. The transition between the use of the two roughness heights in gradual: Below the lower critical mud factor (sc_cmf1) ksSand will be used as the roughness height. Above the upper critical mud factor (sc_cmf2) ksSilt will be used as the roughness height. The physical reasoning behind this is that flow over a bed with large (sandy) grains experiences more friction than flow over a mud bed – hence the bed shear stress over a smooth, muddy bed is lower than over a sandy bed. Sediments therefore more easily deposit on a mud bed than on a sandy bed.

  Effects on model results:
  Transition zones between channels and tidal flats have the tendency to become muddier once the mud content exceeds the critical mud content. This results in much stronger gradients in mud content, and a very pronounced bimodal distribution of the mud content when applying the Soulsby & Clarke method in long-term predictions. When combining van Ledden (2003) with Soulsby & Clarke (2005), larger muddy shoals were able to form in (central parts of) the tidal basin.

  Notes and pitfalls: Note that the formulations of Soulsby & Clarke (2005) do not alter the formulations for erosion or deposition, but the hydrodynamic load (bed shear stress). Application in combination with a buffer model is possible (see van Weerdenburg, 2020 or Appendix 1). The switch between ksSilt and ksSand can be either determined by the mud fraction and the mud thickness (user defined). The former is more realistic when modelling sand-mud mixtures. However, the latter is set as default in Delft3D for backward compatibility reasons. Therefore, in sand-mud modelling, the value should be manually set to sc_mudfactor = #fraction#.

Recommendations for future work

- Previous model runs (not included in this report) with different roughness formulations have shown that the choice for a certain roughness formulation has a large impact on the morphodynamic development in a long-term model simulation, including the distribution of sand and mud in a tidal system. This is caused by a different dependency of the bed roughness on the water depth in different roughness formulations. Hence, the question what roughness formulation to use should be part of the discussion on the right mechanisms to include in sand-mud modelling. We recommend performing a detailed analysis with varying roughness formulation in a future study to determine the effect on the bathymetrical evolution and sand-mud patterns.

- For both the formulations of van Ledden (2003) as those of Soulsby & Clarke (2005), the effect on the morphodynamics will largely be determined by the user-defined threshold parameters. Realistic and careful use of these parameters is thus crucial. The threshold the formulations of van Ledden (2003) has carefully been validated against experimental data in the past (Torfs, 1995). Although the threshold is set at one specific value in Delft3D, it is expected that the transition from one regime to another is more gradual in reality.

It is still largely unknown what realistic thresholds should be for the formulations of Soulsby & Clarke (2005) and this should be addressed in further research. In addition, the value of ksSilt also would need validation with experimental data.

- In addition, a general comparison of the erosion rates with experimental data is recommended, especially under the combined forcing of currents and waves (much less data available).

- In several previous studies it was shown that the sediment composition of Dutch tidal basins and estuaries is characterised by a strong-sand mud segregation, with abrupt transitions between sandy and muddy areas resulting in a bimodal distribution of the mud content. Model simulations have shown that these abrupt transitions can be enhanced when accounting for sand-mud segregation. However, it remains largely unknown how abrupt these transitions exactly are in the field. Detailed field experiments of transects from sandy to muddy areas are needed to study this. It would be interesting to study how these transitions are for field sites with high and low variability of the sediment composition.

- Besides the horizontal transitions that have been analysed in this study, we recommend studying the vertical transitions, i.e. vertically alternating layers of sand and mud. Again, an analysis is recommended on how this is affected by sand-mud interaction, and how this relates to field observations.

- In addition, we recommend analysing and quantifying how sand-mud interaction influences SSC and how this relates to field observations (e.g. a typical Wadden Sea basin with concentration 50 – 100 mg/l).

- In this study, 3 ways to account for sand-mud interaction in Delft3D have been tested in a schematised case. Besides, the module including Soulsby & Clarke has been adapted, see Van Weerdenburg, (2020) or Appendix 1 for the details of the current functionality. The modules appeared to work well in all simulations. The next step is to to further use these modules in case studies, and ideally to thest whether their general functionality and effects on the morphodynamic predictions agree with our findings. It should be noted that neither of the tested modules significantly increased computational times.

6 Conclusions

- Three ways to include (physical) sand-mud interaction are implemented in Delft3D, namely:
    - Making use of β_m, in combination with the van sand transport formulations of van Rijn (1984, 1993, 2007). An increased value of β_m (for 0 to 1 or 3) is used to simulate the effect of an increased threshold for erodibility of sand when the mud content increases.
    - The theory of van Ledden (2003), which accounts for two regimes within sand-mud mixtures, either non-cohesive or cohesive. A critical clay content of 5-10% is found as a threshold between the two regimes, which for Dutch systems corresponds with a critical mud content of around 30%. Sand and mud transport are interdependent within the two regimes.
    - The effect of the bed roughness (depending on the sediment composition) on the bed shear stress acting on sediment particles can be accounted for by using the method of Soulsby & Clarke (2005) to calculate the bed shear-stress generated by waves and currents. The method makes use of a different roughness height for sand and mud (ksSand and ksSilt), and of a (used defined) critical mud content determining the minimum mud content for which the roughness height of mud is used to calculate the bed shear stress.

- Accounting for an increased threshold for erosion with increasing mud content (β_m) has a large effect on erosion rates (especially for high mud content), which largely influences short-term predictions, even in case of large disturbances (when the bed shear stresses are relatively high).
- When using the formulations of van Ledden (2003), short-term erosion rates largely differ for equal simulations with a different critical mud content. Thus, it is concluded that these results are fairly sensitive to this parameter, which should therefore be used with care. The critical mud content is site specific, since it depends on the local clay/silt ratio.
  For muddy sediments that are hard to erode (because of consolidation for instance, with τ_e =0.5-1.0 Pa) maximum erosion rates of mud will occur when the mud content is close to the critical mud content. However, for soft mud sediments (τ_e =0.05-0.1 Pa), mud erosion rates are maximum in the fully mud regime. This is because in the first case (consolidated mud), $\tau_{,cr}$ is in the cohesive regime larger than in the non-cohesive regime, while in the second case (soft mud) it is lower.
  Accounting for sand-mud interaction as defined by van Ledden (2003) in long-term predictions, the basin channels evolved less far into the basin. Besides, a relatively sharp transition was observed from areas with a low mud fraction to areas with a high mud fraction, where the basin becomes shallower.
- Short-term simulations with Soulsby & Clarke (2005) sand-mud interaction are not very sensitive to the settings for the transition zone between ksSilt and ksSand, although this sensitivity increases with decreasing value for ksSilt.
  The influence of the mud content on the bottom roughness in the Soulsby & Clarke method only affects the bed shear stress if the mud content is higher than 30% (start of the transition zone). Above 30%, the bed roughness starts to decrease, such that the hydrodynamic conditions lead to lower bed shear stresses. Transition zones between channels and tidal flats thus have the tendency to become muddier once the mud content exceeds 30%, resulting in stronger gradients in mud content when applying the Soulsby & Clarke method in long-term predictions.

- Changing the settings for sand-mud interaction largely affects the predicted long-term morphological evolution. This shows the sensitivity of the results to the user defined

settings. We have shown that model performance increases with respect to the bed sediment composition. The question remains whether this is also the case for the bathymetric development. A strong sand-mud segregation characterises the bed composition in Dutch tidal basins and estuaries. This leads to beds that are preferably either predominantly sandy or muddy (revealed by a bimodal distribution of the mud content in the bed). Modelling simulations including the effect of the hydraulic roughness depending on the mud content (making use of Soulsby & Clarke, 2005) are able to reproduce the bimodal character and show sharp transitions between the sandy and muddy areas.

- With increasing mud availability, the right peak of the bimodality becomes larger, meaning that more sites become muddy. This is either by increasing the SSC at the boundaries or by increasing the initial mud content in the sediment bed. Vice versa, the left peak becomes larger (more sites becoming sandy) with decreasing mud content. However, in all cases the bimodality remains, and a strong sand-mud segregation is observed in all cases.
  Not only the sediment composition is affected, but also the bathymetry. In general, tidal flats become larger and higher with increasing mud availability. These results show that this system's evolution is largely steered by the sediment availability.

Bibliography

Bisschop, F. (1993). *Erosieproeven op zand met variatie in doorlatendheid (in Dutch) (Combinatie Speurwerk Bagger- techniek BAGT510 No. J714).* Delft: WL|Delft Hydraulics.

Braat, L., van Kessel, T., Leuven, J. R., & Kleinhans, M. G. (2017). Effects of mud supply on large-scale estuary morphology and development over centuries to millennia. *Earth Surface Dynamics, 5(4)*, 617–652.

Colina Alonso, A. (2020). *Evolutie van het bodemslib in de Waddenzee: Data analyse.* Delft: Deltares report 11205229-001-ZKS-0003, 42 pp.

Colina Alonso, A., van Weerdenburg, R., van Maren, B., & Huismans, Y. (2020). *Modelling sand-mud interaction in Delft3D.* Deltares report.

De Bake, D. (2000). *Zand-slibsegregatie in de Westerscheldc (in Dutch).* Delft: Msc. thesis, Delft University of Technology.

de Glopper, R. (1967). Over de bodemgesteldheid van het waddengebied. *Van Zee tot Land*, 5-61.

Deltares. (2018). *Delft3D-FLOW - User Manual (Version 3.15).*

Engelund, F., & Hansen, E. (1967). *A monograph on sediment transport in alluvial streams, Tech. Rep, .* Copenhagen, Denmark: Teknsik Vorlag.

Grabowski, R., Droppo, I., & Wharton, G. (2011). Erodibility of cohesive sediment: The importance of sediment properties. *Earth-Science Reviews 105*, 101–120.

Herman, P. M., van Kessel, T., Vroom, J., Dankers, P., Cleveringa, J., de Vries, B., & Villars, N. (2018). *Mud dynamics in the Wadden Sea: towards a conceptual model.* Delft: Deltares.

Jacobs, W. (2011). *Sand-mud erosion from a soil mechanical perspective (PhD thesis).* Delft: Delft University of Technology.

Malarkey, J., & Davies, A. (2012). A simple procedure for calculating the mean and maximum bed stress under wave and current conditions for rough turbulent flow based on Soulsby and Clarke's (2005) method. *Computers & Geosciences*(43), 101-107.

McLaren, P. (1994). *Sediment Transport in the Western Scheldt between Baarland and Rupelmonde.* Cambridge, UK: GeoSea report, GeoSea Consulting.

Mitchener, H., & Torfs, H. (1996). Erosion of mud/sand mixtures. . *Coastal Engineering 29*, 1–25.

Scheel, F. (2012). *Simulating and classifying large-scale spatial sand-mud segregation using a process-based model for a tidal inlet system. A process-based assessment on the relation between different forcing conditions and large-scale spatial sand-mud segregation. .* MSc-thesis Delft University of Technology. (http://repository.tudelft.nl) .

Soulsby, R. (1983). The bottom boundary layer of shelf seas. In B. Johns, *Physical Oceanography of Coastal and Shelf Seas* (pp. 189-266). Amsterdam: Elsevier.

Soulsby, R. (1997). *Dynamics of Marine Sands. A Manual for Practical Applications.* London.: Thomas Telford Publishing.

Soulsby, R., & Clarke, S. (2005). *Bed Shear-stresses Under Combined Waves and Currents on Smooth and Rough Beds.* Defra project FD1905 (EstProc), Report TR 137.

Torfs, H. (1995). *Erosion of mud/sand mixtures.* Leuven: PhD Thesis, Katholieke Universiteit Leuven.

Torfs, H. (1995). *Erosion of mud/sand mixtures. Ph.D. Thesis,.* Leuven: Katholieke Universiteit Leuven.

Van de Koppel, J., Herman, P., Thoolen, P., & Heip, C. (2001). Do alternate stable states occur in natural ecosystems? Evidence from a tidal flat. *Ecology 82*, 3449-3461.

van Kessel, T., Spruyt-de Boer, A., van der Werf, J., Sittoni, L., van Prooijen, B., & Winterwerp, H. (2012). *Bed module for sand-mud mixtures, in framework of BwN project NTW 1.3 mud dynamics.* Delft: Deltares.

Van Ledden, M. (2003). *Sand-mud segregation in estuaries and tidal basins.* PhD thesis; Delft University of Technology.

van Ledden, M., van Kesteren, W. G., & Winterwerp, J. C. (2004). A conceptual framework for the erosion behaviour of sand–mud mixtures. *Continental Shelf Research 24*.

Van Ledden, M., Van Kesteren, W., & Winterwerp, J. (2004). A conceptual framework for the erosion behaviour of sand and mud mixtures. *Cont. Shelf Res., 24*, 1–11.

Van Rijn, L. (1984). Sediment transport, Part I: bed load transport. *Journal of Hydraulic Engineering, 100*(10), 1431-1456.

Van Rijn, L. (1993). *Principles of sediment transport in rivers, estuaries and coastal seas.* Amsterdam, the Netherlands: Aqua publications.

Van Rijn, L. (1993). Principles of Sediment Transport in Rivers, Estuaries and Coastal Seas. *Aqua Publications, The Netherlands*.

Van Rijn, L. (2007). Unified View of Sediment Transport by Currents and Waves. I: Initiation of Motion, Bed Roughness, and Bed-Load Transport. *Journal of Hydraulic Engineering, 133*(6), 649-667.

van Rijn, L., Colina Alonso, A., & van Maren, D. (2020). *Literature Review MUSA: on the Interaction between Mud and Sand.* MUSA Project.

Van Straaten, L., & Kuenen, P. (1957). Accumulation of fine grained sediments in the Dutch Wadden Sea. *Geologie en Mijnbouw, 19*, 329-354.

Van Weerdenburg, R. (2020). *Application of Soulsby & Clarke (2005) in Delft3D.* Deltares memo.

Whitehouse, R., Soulsby, R. R., & Mitchener, H. (2000). *Dynamics of estuarine muds. A manual for practical applications. .* London: Thomas Telford Publishing.

Winterwerp, J. C. (1989). *Flow induced erosion of cohesive beds. A literature survey In Cohesive Sediments (Rep. 25).* Delft: WL|Delft Hydraulics and Rijkswaterstaat.

Winterwerp, J. C., & van Kesteren, W. G. (2004). *Introduction to the phyics of cohesive sediment in the marine environment.* Amsterdam: Elsevier.

Zwarts, L. (2004). *Bodemgesteldheid en mechanische kokkelvisserij in de Waddenzee.* Rapport RIZA.

Appendices

A.1 Appendix 1: Memo - Application of Soulsby & Clarke (2005) in Delft3D

A.1.1 Introduction

Recently, different modules to account for interaction between sand and mud particles in the sediment bed in Delft3D and D-Flow FM have been investigated within the scope of the SO Resilient Ecosystems program. As part of that investigation, the opportunities to apply the bed roughness computations according to Soulsby & Clarke (2005) have been improved and extended. This memo is meant to give an overview of these opportunities and to inform users on how to apply these in their models.

The Soulsby & Clarke (2005) module can be applied in both Delft3D and D-Flow FM. An example of the application in a tidal inlet system and an investigation of the parameter space are discussed in Colina Alonso et al. (2020).

A.1.2 Framework

The algorithm by Soulsby & Clarke (2005) (SC05) can be used to compute the bed shear stress under the combined effect of waves and currents, in which the skin friction is dependent on the composition of the sediment bed. The dependence on the sediment composition is discretized in Delft3D and D-Flow FM by using a different roughness height for sandy beds on the one hand and for muddy sediment beds on the other hand. The SC05 method may thus be particularly attractive when modelling the transport of both sand and mud fractions.

When applying the SC05 method in Delft3D or D-Flow FM, the bed shear stress for currents (τ_{hydro}) is computed with the form roughness. This form roughness is based on a user-prescribed uniform or spatially varying Chézy, Manning, or Nikuradse coefficient. However, a skin friction instead of a form roughness is used to compute the bed shear stresses (τ_{morph}) based on which the resuspension of sediment is determined. The physical argument for this distinction is that sediment transport rates are determined primarily by the local bed roughness, and not the large-scale roughness resulting from bed forms. Also, flow over a bed with large (sandy) grains experiences more friction than flow over a mud bed – hence the bed shear stress over a smooth, muddy bed is lower than over a sandy bed. Sediments therefore more easily deposit on a mud bed than on a sandy bed.

SC05 provides the opportunity to (1) disconnect the bed shear stress on sediment particles from the bed shear stress experienced by the flow, and (2) differentiate between the bed shear stress over muddy beds and sandy beds. This is especially useful for morphodynamic- and sediment transport modelling in mixed sand-mud environments, in which the resuspension and transport of sediment may be stirred by the local skin friction rather than the form roughness.

A.1.3 Application

Bed shear stresses are computed in Delft3D according to the theory by SC05 if `bsskin = true` in the `[SedimentOverall]` block of the sed-file. In the algorithm the roughness height may vary between `ksSand` and `ksSilt`, depending on the (relative) amount of mud in the active layer. Several keywords may be used to adjust the computations since revision 65780 of the Delft3D source code. These keywords should be specified in the `[SedimentOverall]` block of the sed-file.

- `ksSilt` is the roughness height (in [m]) in case the top layer of the sediment bed mainly consists of mud particles (i.e. smooth beds).
- `ksSand` is the roughness height (in [m]) in case the top layer of the sediment bed mainly consists of sand particles (i.e. rough beds).
- `sc_mudfactor` determines whether the total mud thickness in the active layer or the mud fraction (i.e. by mass) determines the switch between `ksSilt` and `ksSand`. The value should be `#thickness#` or `#fraction#`. The default is `#thickness#` for backward compatibility reasons.
  In mud models (i.e. without simulating a sand fraction) the mud fraction is always equal to unity; therefore setting `sc_mudfactor = #thickness#` is the only way to change the bottom roughness depending on the amount of mud present in the bed. In sand-mud modelling, the value should be manually set to `sc_mudfactor = #fraction#`.
- `sc_cmf1` is the lower critical mud factor. Below this value `ksSand` will be used as the roughness height. The default value is 0.01 (see Figure A.1).
- `sc_cmf2` is the upper critical mud factor. Above this value `ksSilt` will be used as the roughness height. The default value is 0.01 (see Figure A.1).

Between `sc_cmf1` and `sc_cmf2`, the roughness height will gradually change from `ksSilt` into `ksSand` (or vice versa, see Figure A.2). By increasing the difference between `sc_cmf1` and `sc_cmf2` the transition becomes more gradual. The default settings are included in Figure A.1.

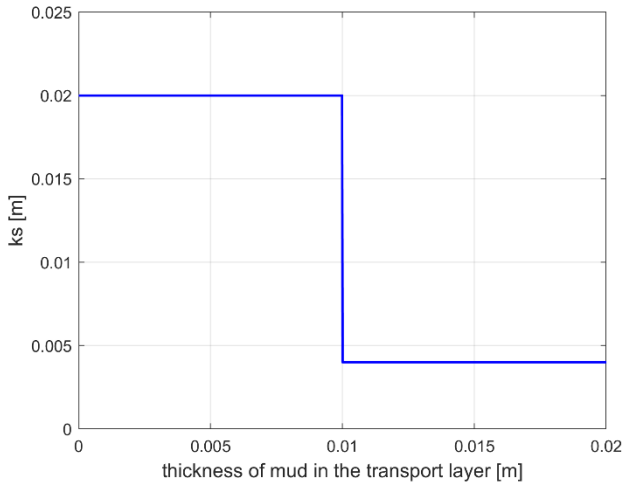

Figure A.1: Roughness height with default settings (`sc_mudfactor = #thickness#, sc_cmf1 = 0.01` and `sc_cmf2 = 0.01`) and `ksSand = 0.02 m` and `ksSilt = 0.004 m`.

An example of the keywords in the `[SedimentOverall]` block of the sed-file is given below. The listed settings are used in Figure A.2.

```
[SedimentOverall]
 Cref            = 1600.0          [kg/m3]
 IopSus          = 0
 bsskin          = true
 sc_mudfactor    = #fraction#
 sc_cmf1         = 0.3
 sc_cmf2         = 0.5
 kssilt          = 0.004           [m]
 kssand          = 0.02            [m]
```

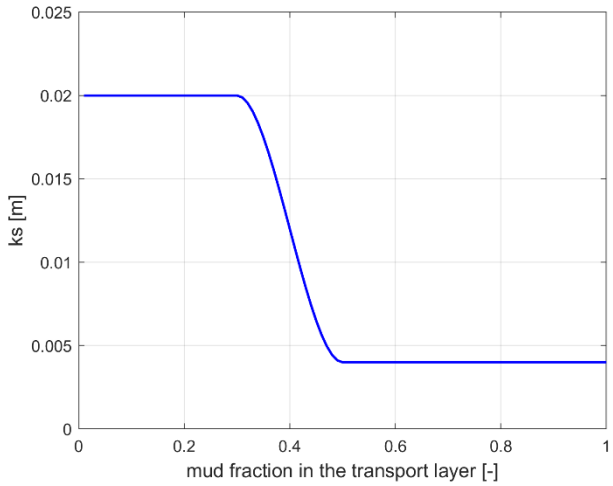

Figure A.2: Roughness height with settings `sc_mudfactor = #fraction#, sc_cmf1 = 0.3, sc_cmf2 = 0.5, ksSand = 0.02 m` and `ksSilt = 0.004 m`.

A.1.4 Buffer model

If the sediment bed contains a flufflayer, the SC05 module will account for this in determining the bed roughness. If the flufflayer is sufficiently thick at a certain location, `ksSilt` is used as the local bed roughness (i.e. independent from the value set for `sc_mudfactor`). Users may define when they consider the bed completely covered by the flufflayer by setting a threshold value. This threshold value is defined as a fraction of `ParFluff1/ParFluff0`, where `ParFluff1 [1/s]` is the first order erosion parameter of the fluff layer and `ParFluff0 [kg/m²/s]` is the zeroth order erosion parameter of the flufflayer. The threshold fraction is named `CritFluffFactor` and should be listed in the `[SedimentOverall]` block of the sed-file. The default value of `CritFluffFactor` is 0.5. So if the mass in the flufflayer is larger than `CritFluffFactor*ParFluff1/ParFluff0`, `ksSilt` is considered the local roughness height. In case multiple mud fractions are simulated, `ksSilt` is used if the total mass of mud in the fluff layer exceeds `CritFluffFactor*ParFluff1/ParFluff0`.

In case there is no mass in the flufflayer, the roughness height (i.e. either `ksSand` or `ksSilt`) will be based on the sediment composition in the first buffer layer (i.e. using `sc_mudfactor`, `sc_cmf1`, and `sc_cmf2`). If the flufflayer contains mass, but not enough to consider the flufflayer to cover the entire bed, the roughness height is based on a linear interpolation between the roughness height of the first buffer layer (i.e. either `ksSand` or `ksSilt`) and the roughness height of the flufflayer (i.e. `ksSilt`). This interpolation is illustrated in Figure A.3 for the settings listed below. The mass in the flufflayer is included as a fraction of `ParFluff0/ParFluff1`.

```
[SedimentOverall]
 bsskin          = true
 sc_mudfactor    = #fraction#
 sc_cmf1         = 0.3
 sc_cmf2         = 0.5
 kssilt          = 0.004           [m]
 kssand          = 0.02            [m]
 critflufffactor = 0.6
```

In case the buffer layer mainly consists of mud, `ksSilt` is going to be applied as the roughness height independent on the amount of mass in the flufflayer. In case the buffer layer is particularly sandy, the roughness height reduces from `ksSand` to `ksSilt` if the amount of mass in the flufflayer increases.

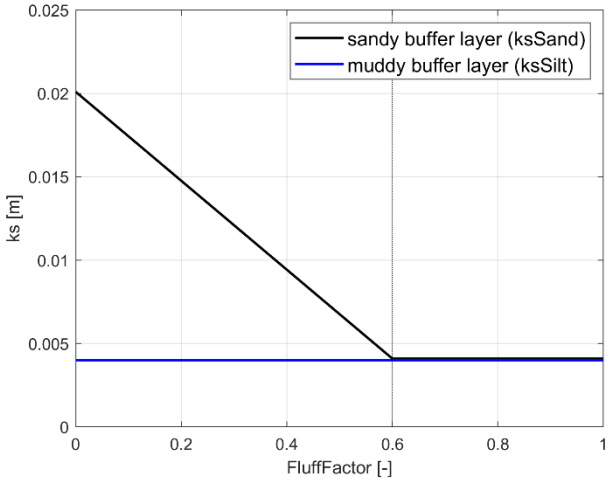

Figure A.3: Roughness height depending on the mass in the fluff layer, which is given as FluffFactor = Mass / (ParFluff0 / ParFluff1). The critical mass above which the roughness height is no longer depending on the sediment composition in the buffer layer is here set to CritFluffFactor = 0.6.

A.1.5 Additional remarks

This memo was written to inform users of Delft3D and D-Flow FM about the opportunity to use the SC05 method in sand-mud modelling and to help them to apply the method. In case there are any further questions or remarks, do not hesitate to contact Roy van Weerdenburg (Roy.vanWeerdenburg@Deltares.nl) or Bas van Maren (Bas.vanMaren@Deltares.nl).

A.2 Figures on the long-term morphodynamic development

A.2.1 Morphology and bed composition

Van Rijn (1993), $\beta_m = 0$

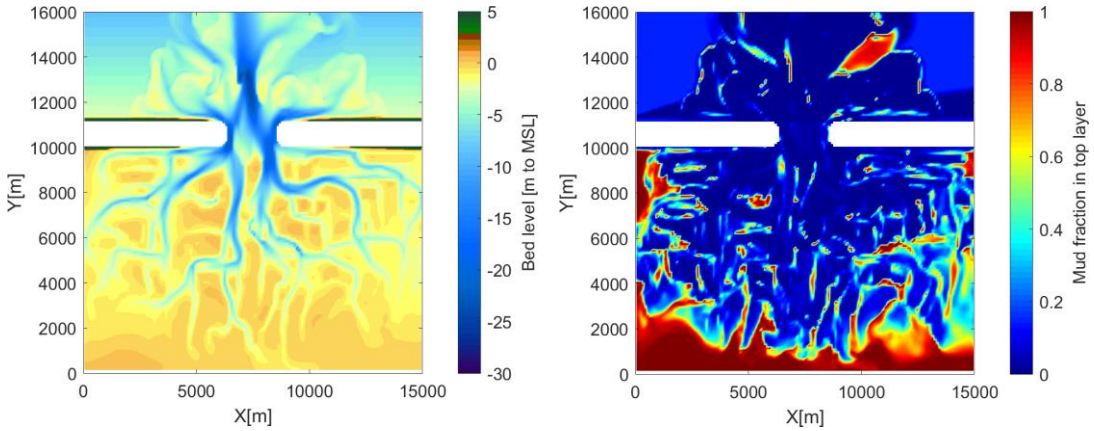

Van Rijn (1993), $\beta_m = 1$

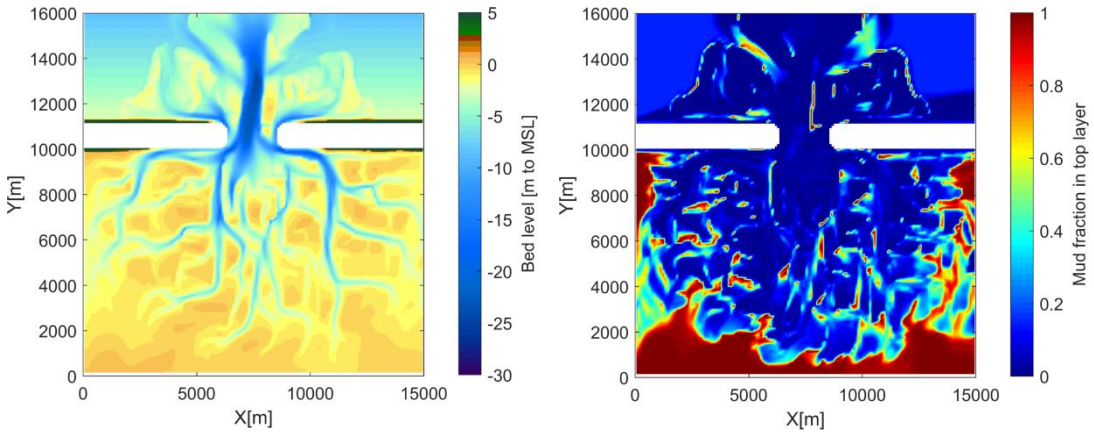

Van Rijn (1993), $\beta_m = 3$

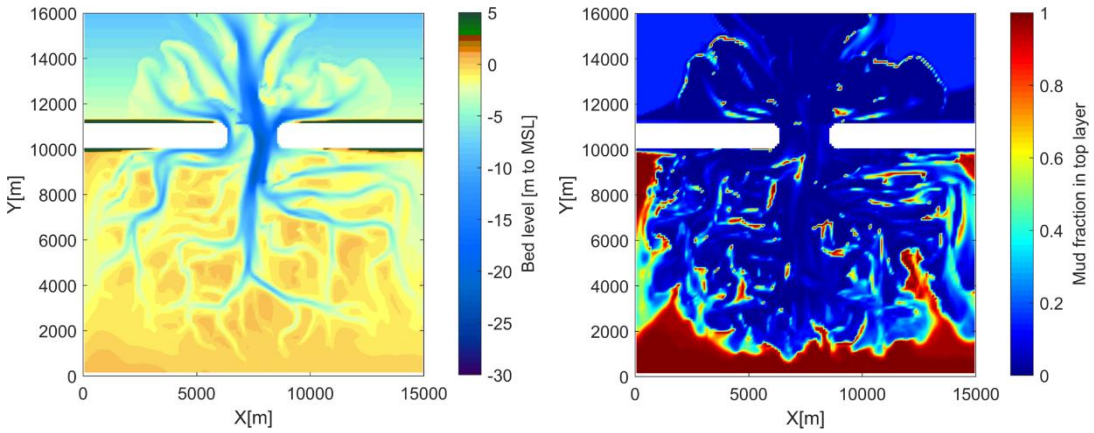

Van Ledden, β_m = 1

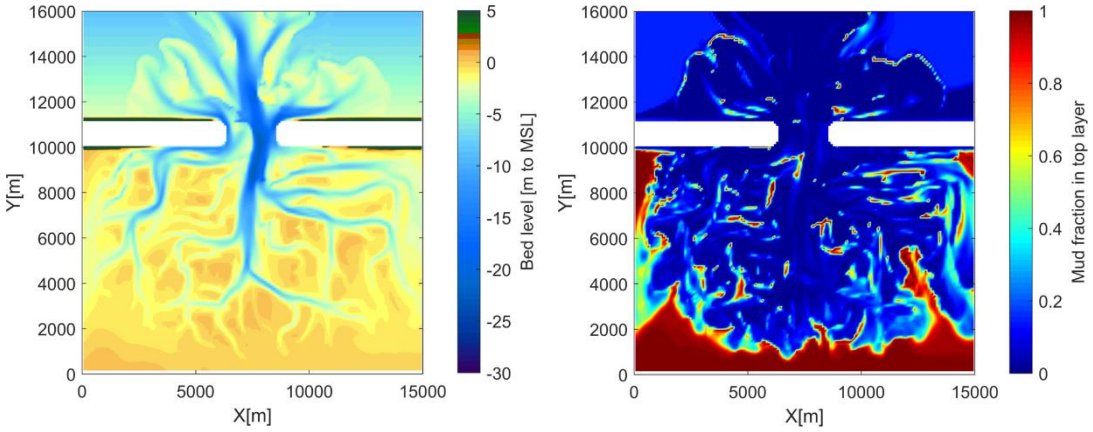

Soulsby & Clarke, β_m = 0

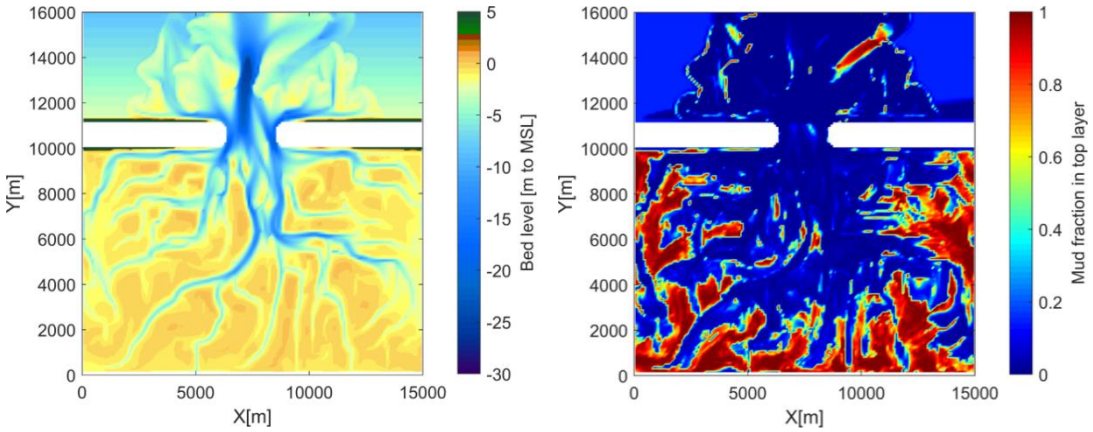

Van Ledden, Soulsby & Clarke, β_m = 1

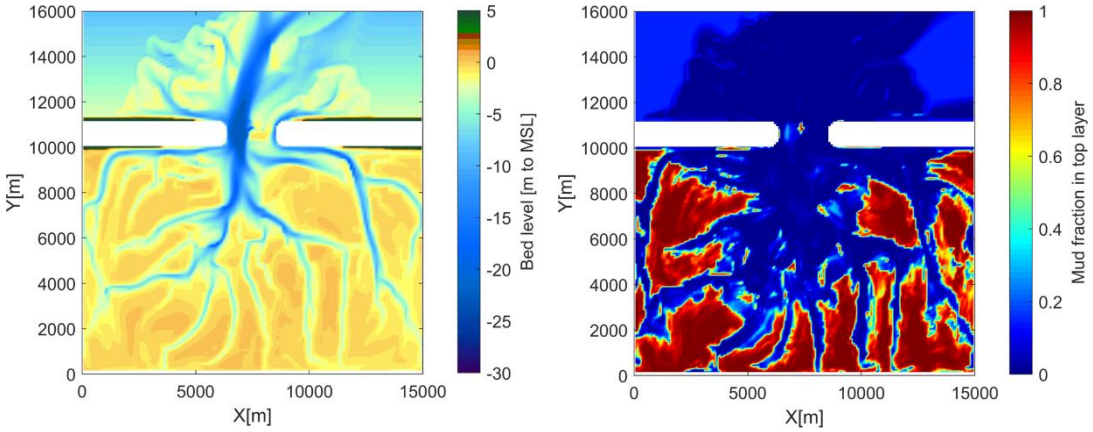

A.2.2 Sand-mud segregation

Van Rijn (1993), β_m = 0

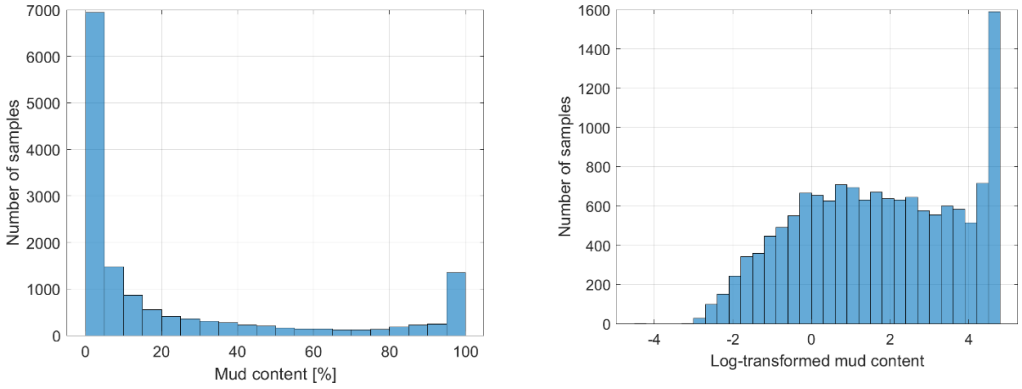

Van Rijn (1993), β_m = 1

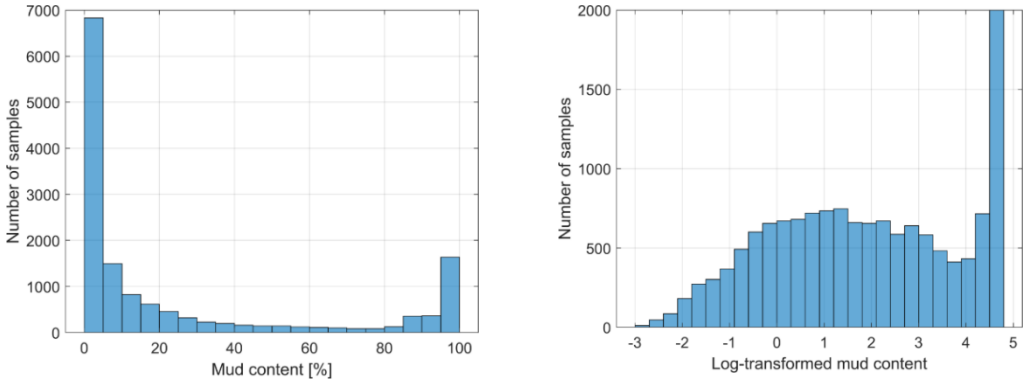

Van Rijn (1993), β_m = 3

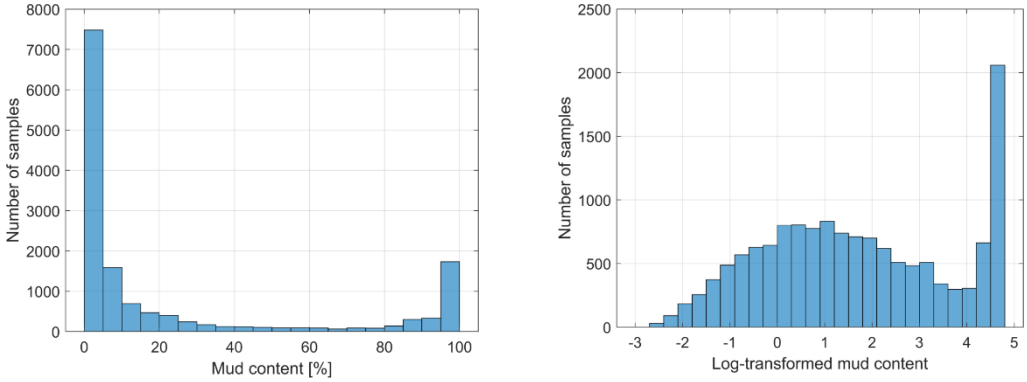

Van Ledden, β_m = 1

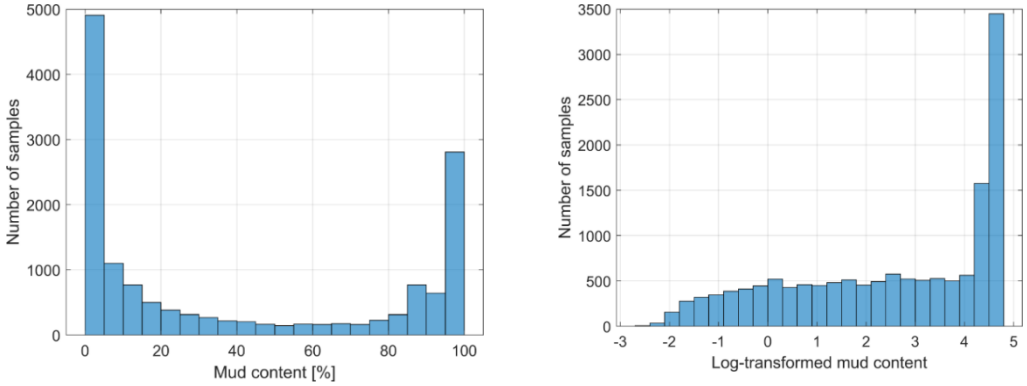

Soulsby & Clarke, $\beta_m = 0$

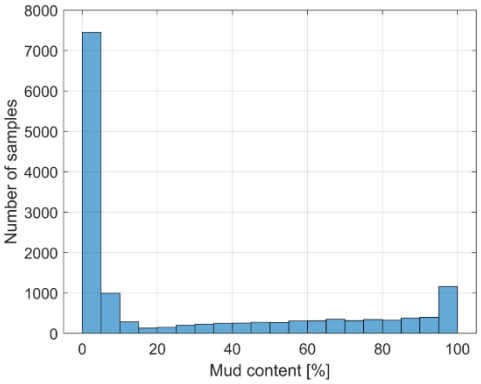

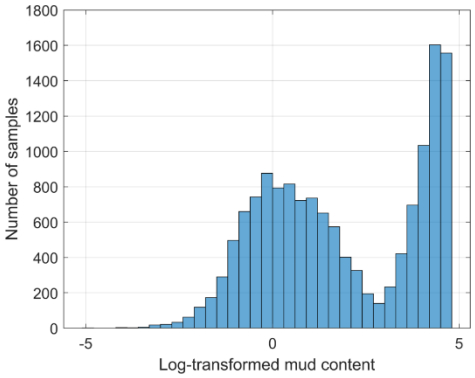

Van Ledden, Soulsby & Clarke, $\beta_m = 1$

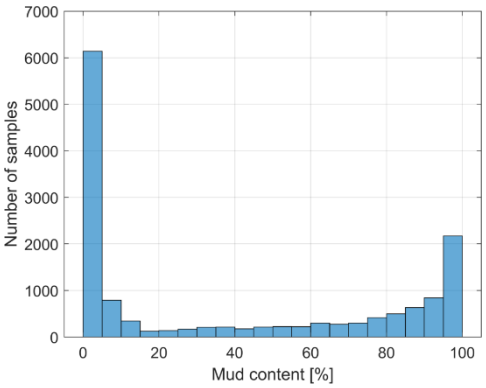

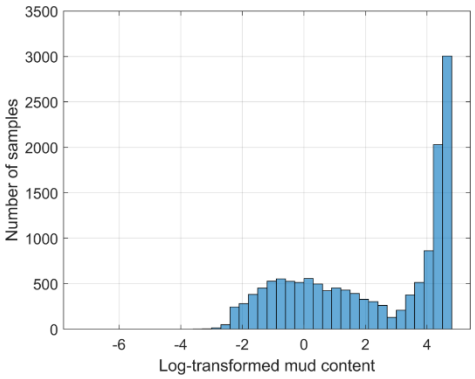

A.2.3 Dependency of mud content and bed shear stress

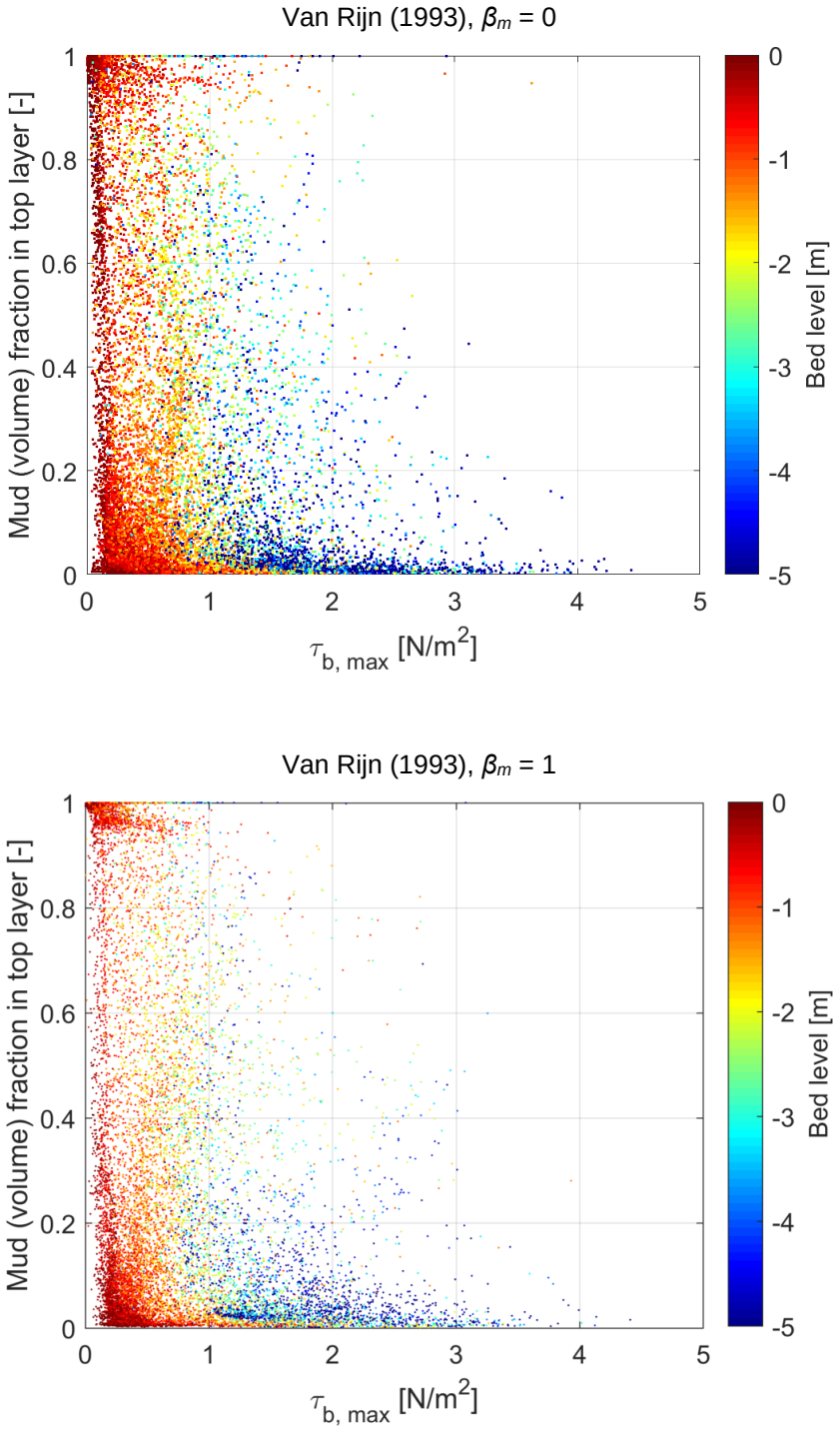

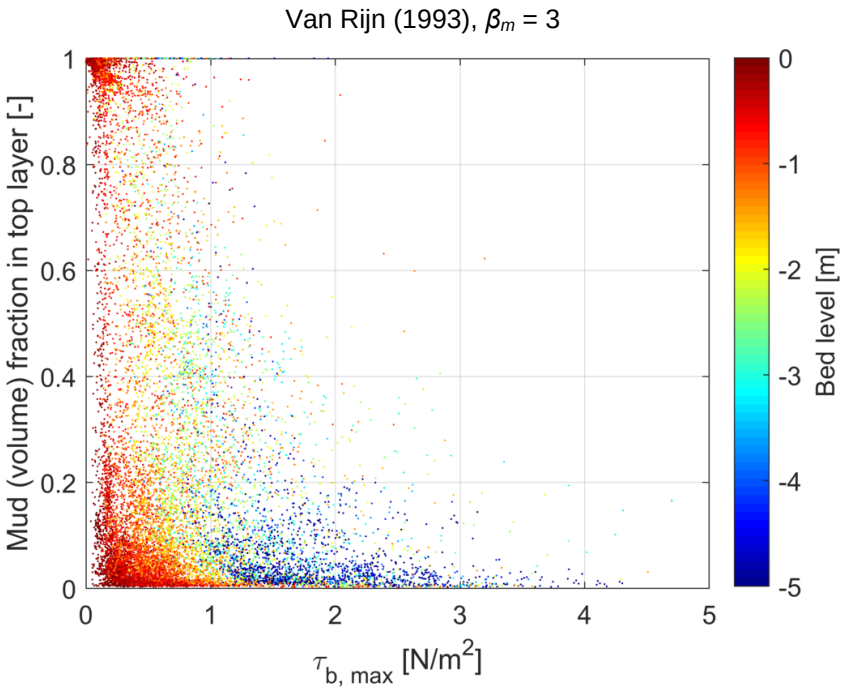
Van Rijn (1993), β_m = 3
Mud (volume) fraction in top layer [-]
$\tau_{b,\,max}$ [N/m^2]
Bed level [m]
0
0.2
0.4
0.6
0.8
1
0
1
2
3
4
5
-1
-2
-3
-4
-5

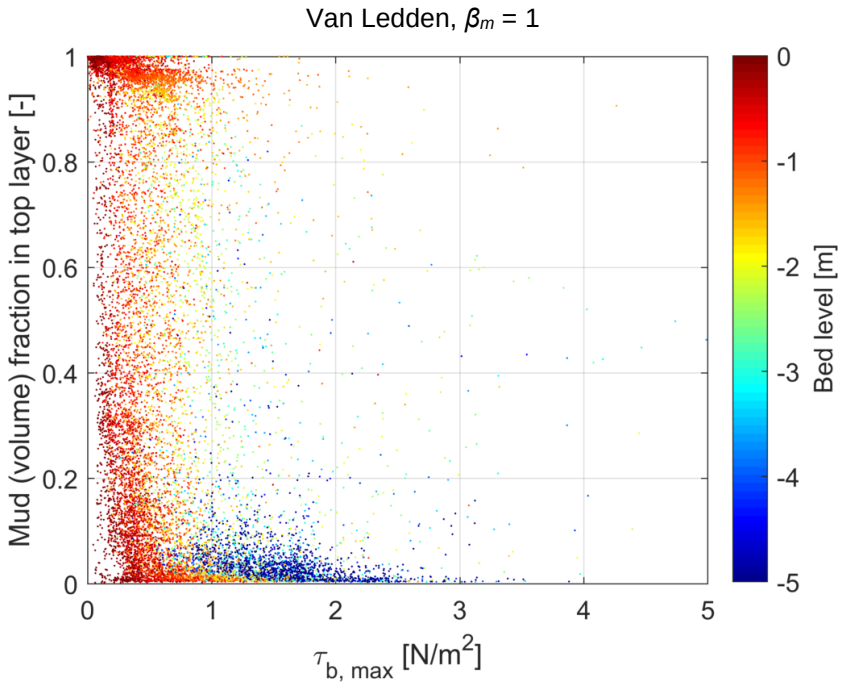
Van Ledden, β_m = 1
Mud (volume) fraction in top layer [-]
$\tau_{b,\,max}$ [N/m^2]
Bed level [m]
0
0.2
0.4
0.6
0.8
1
0
1
2
3
4
5
-1
-2
-3
-4
-5

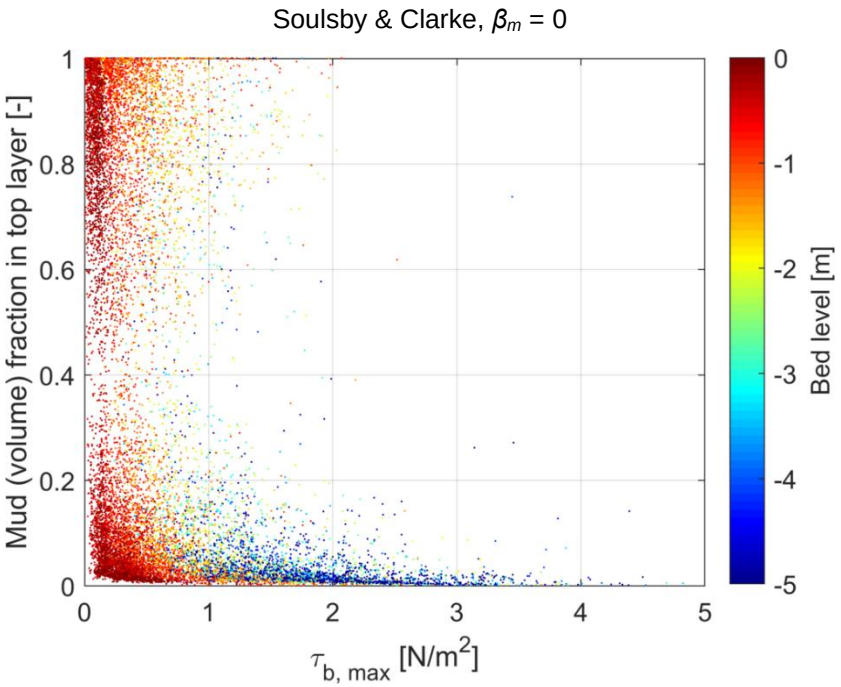
Soulsby & Clarke, β_m = 0
Mud (volume) fraction in top layer [-]
$\tau_{b,\,max}$ [N/m^2]
Bed level [m]
0
0.2
0.4
0.6
0.8
1
0
1
2
3
4
5
-1
-2
-3
-4
-5

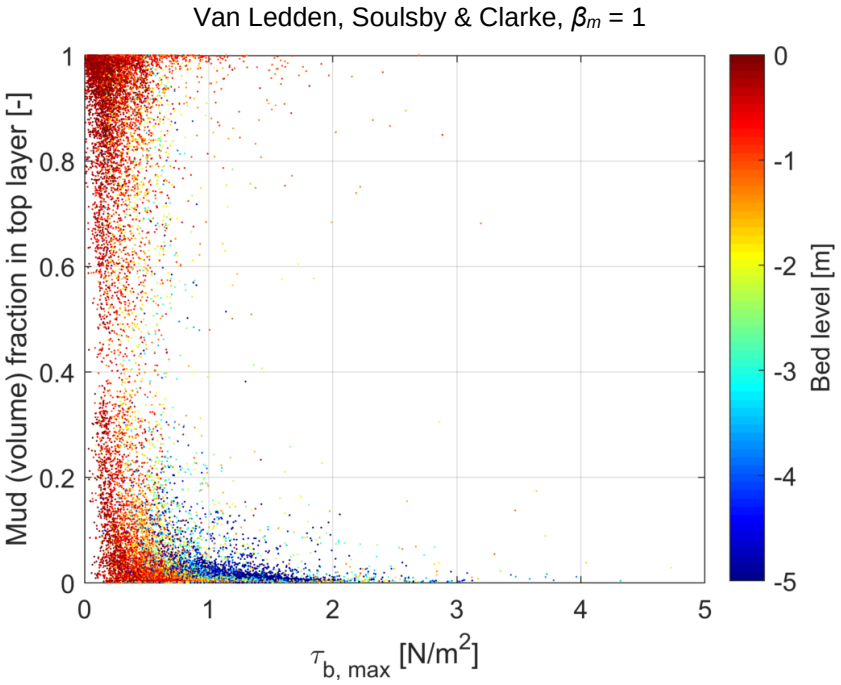
Van Ledden, Soulsby & Clarke, β_m = 1
Mud (volume) fraction in top layer [-]
$\tau_{b,\,max}$ [N/m^2]
Bed level [m]
0
0.2
0.4
0.6
0.8
1
0
1
2
3
4
5
-1
-2
-3
-4
-5

Deltares is een onafhankelijk kennisinstituut voor toegepast onderzoek op het gebied van water en ondergrond. Wereldwijd werken we aan slimme oplossingen voor mens, milieu en maatschappij.

Deltares

www.deltares.nl